A catastrophe model for the stability of ships.

E.C. Zeeman.

To appear in
Proc. Esc. Lat.-Am. Math. 3 (1976)
I.M.P.A., Rio de Janeiro, Brazil.

Mathematics Institute
University of Warwick
Coventry.

A CATASTROPHE MODEL FOR THE STABILITY OF SHIPS

E.C. Zeeman

1. INTRODUCTION.

Catastrophe theory provides a new way of looking at the statics of a ship, and this in turn lends a new simplicity to the global non-linear dynamics. The weight of the ship and the position of the centre of gravity are taken as parameters. Then the set of equilibrium positions form a smooth manifold that maps onto the parameter space. It is the singularities of this map that are recognisable as elementary catastrophes.

For example heeling and capsizing are fold catastrophes. At the metacentre there is a cusp catastrophe. The point of inflexion of the lever arm curve is caused by another cusp catastrophe. The increased likelihood of capsizing when overloaded, or when the crest of a wave is amidships, is due to a swallowtail catastrophe. The evolution of hull shape from canoe to modern ship is characterised by a butterfly catastrophe. On the metacentric locus there are also hyperbolic umbilic catastrophes. The sudden onset of heavy rolling due to non-linear resonance with the wave is a dynamic fold catastrophe.

For the naval architect this approach in terms of canonical forms offers a qualitative geometry that is complementary to the classical approach [2,3,9,11]. Whether or not such formulation will be of any use remains to be seen, because to make quantitative predictions it is still necessary to choose coordinates and approximations as in the classical theory. However as a general principle it is always advantageous to retain the dynamics in a conceptually simple form for as long as possible, so that the important qualitative features can be kept in the forefront of the

mind unobscured by detail, allowing the eventual approximation to be tailored to the job on hand. Catastrophe theory should be used like the zoom lens on a microscope, for gaining a global view of the problem, and thus enhancing the discrimination with which one selects the necessary tool from classical mathematics to zoom in and solve it.

For the mathematician the interest of this example lies in the rich variety of the mathematics that it brings together; it is a prototype revealing catastrophe theory as a natural generalisation of Hamiltonian dynamics. Besides having a parameter space, an elementary catastrophe model has a state space, a potential, and a dynamic minimising the potential. Here the state space is the usual phase space of Hamiltonian dynamics, namely the cotangent bundle of the configuration space of the ship, while the potential is none other than the Hamiltonian, which is a Lyapunov function for, and therefore locally minimised by, the Hamiltonian flow with any type of damping. The subtlety comes from the bifurcations of the dynamic over the parameter space, which are governed by the elementary catastrophes in the evolute of the buoyancy locus.

We begin the paper by giving in Sections 2 - 6 a brief elementary sketch of the classical linear theory of ship motions, partly for the benefit of readers unfamiliar with the topic, and partly to see later how the model generalises it. The reader familiar with the linear theory is recommended to proceed at once to Section 7, where we describe the significance of the geometry. The model itself is introduced in Section 10, at first for rolling only, and then successively enlarged to include pitching, heaving and loading. At the end in Section 14 we place the treatment in its proper group-theoretical setting.

An unsolved problem is how best to incorporate into the model the forcing terms of wind and wave, so as to prove

global existence theorems concerning induced oscillations, resonance and capsizing. The model already sheds some light on capsizing. In the conclusion we tentatively suggest two areas for further exploration.

CONTENTS

2. LINEAR THEORY OF ROLLING.

The classical linear theory of how a ship behaves like a pendulum hanging from the metacentre dates back to Euler [7] in 1737 and Bouguer [4] in 1746. For simplicity we begin by confining ourselves to the artificial 2-dimensional problem of rolling only. When we come to the catastrophe model, the notation will allow us to generalise with ease to the full 3-dimensional situation.

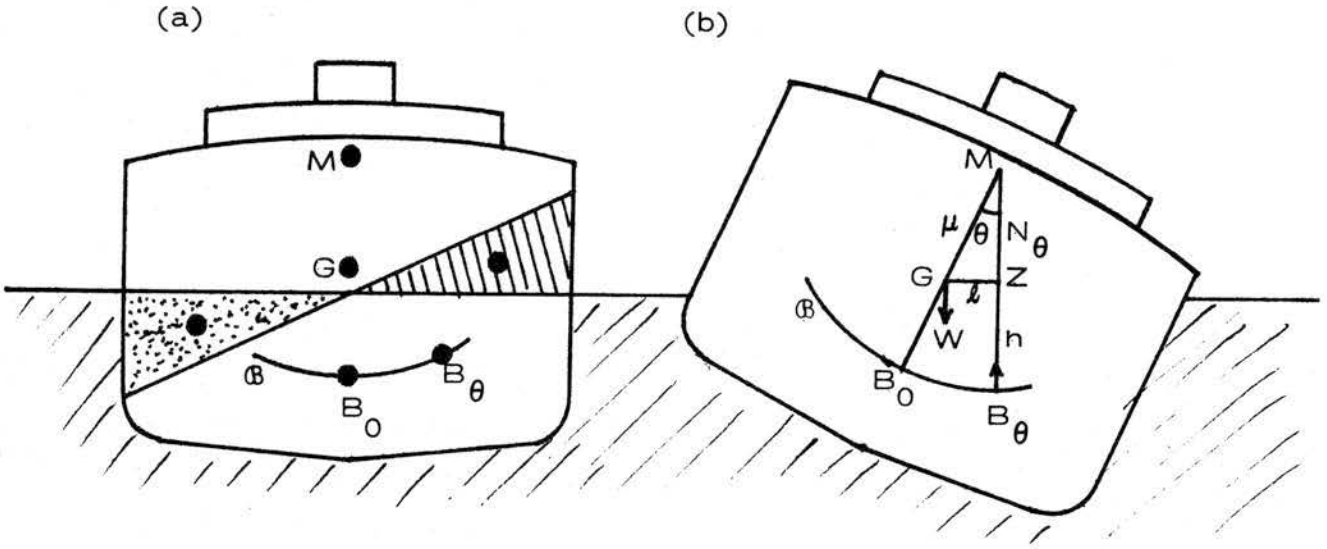

Figure 1. The buoyancy locus and metacentre.

Let G = centre of gravity of ship.

B_0 = centre of buoyancy when ship floats vertically
= centre of gravity of water displaced.

B_θ = centre of buoyancy when ship is at angle θ.

$\mathfrak{B}$ = <u>buoyancy locus</u> = $\{B_\theta;\ -\pi < \theta \leq \pi\}$

N_θ = normal to $\mathfrak{B}$ at B_θ.

M = <u>metacentre</u> = centre of curvature of $\mathfrak{B}$ at B_0.

μ = GM = <u>metacentric height.</u>

Lemma 1. $\mathcal{B}$ is a convex closed curve. When the ship is heeled at angle θ, the normal N_θ is vertical.

Proof. Let A_θ denote the water displaced at angle θ. The area of A_θ is independent of θ, since by Archimedes principle the weight of water displaced equals that of the ship. A_θ is obtained from A_0 by adding the immersed wedge, shown shaded in Figure 1, and subtracting the emerged wedge, shown dotted. Since the wedges have equal area, B_0B_θ is parallel to the line joining the centres of gravity of the two wedges. As $\theta \to 0$ this line tends to the horizontal in Figure 1(a), and hence the tangent to $\mathcal{B}$ at B_0 is horizontal in Figure 1(a). The above argument is independent of the symmetry at $\theta = 0$, and hence applies to any θ. Therefore the tangent to $\mathcal{B}$ at B_θ is horizontal in Figure 1(b), and hence the normal N_θ is vertical.

For small θ, the inclination of B_0B_θ to the horizontal has the same sign as θ, and hence the curvature of $\mathcal{B}$ at B_0 is upwards. The same argument applies to any θ, and hence $\mathcal{B}$ is convex.

Corollary. For small θ, the buoyancy force passes approximately through the metacentre M.

Proof. The buoyancy force acts vertically upwards at B_θ, and therefore along the normal N_θ. For small θ the normals pass approximately through the centre of curvature, M. In fact since B_0 is a point of symmetry of $\mathcal{B}$, the distance from M to N_θ is of order θ^3.

Remark. For the 3-dimensional problem the same result holds, with the proviso that $\mathcal{B}$ is now a convex closed surface; the proof is the same. Note that the result is independent of the shape of hull, and holds not only for ordinary ships but also for catamarans and icebergs, for example.

The righting couple in Figure 1(b) consists of the weight W of the ship acting downwards at G, and the buoyancy force W acting

upwards at B_θ. Let ℓ denote that lever arm of this couple :

ℓ = distance from G to N_θ

= GZ, in Figure 1(b) ,

where Z is the foot of the perpendicular from G to N_θ. Newton's law of motion gives :

$$I\ddot{\theta} = -W\ell \quad \ldots\ldots\ldots\ldots\ldots\ldots \quad (1)$$

where I is the moment of inertia of the ship (and the entrained water) about G. From the Corollary to Lemma 1 and Figure 1(b),

$\ell = \mu \sin\theta$, to second order in θ,

$= \mu\theta$, again to second order.

Hence the approximate linear equation is

$$I\ddot{\theta} = -W\mu\theta. \quad \ldots\ldots\ldots\ldots\ldots\ldots \quad (2)$$

This has rolling solution

$$\theta = \theta_o \cos \frac{2\pi t}{T} \quad \ldots\ldots\ldots\ldots\ldots \quad (3)$$

where θ_o is the amplitude and T the period of the roll. The amplitude is arbitrary, and the period is given by

$$T = 2\pi\sqrt{\frac{I}{W\mu}} . \quad \ldots\ldots\ldots\ldots\ldots \quad (4)$$

The viscosity of the water has a damping effect, and the simplest way to put this into the dynamics is to add a small damping term $2\varepsilon\dot{\theta}$ to equation (2), where ε is a small positive constant :

$$\ddot{\theta} + 2\varepsilon\dot{\theta} + \frac{W\mu}{I}\theta = 0 . \quad \ldots\ldots\ldots \quad (5)$$

This has the effect of multiplying the solution (3) by a decay factor $e^{-\varepsilon t}$, and lengthening the period by a factor of order ε^2, which we can ignore.

3. QUANTITATIVE ESTIMATES.

By (2) the larger the metacentric height the more stable is the ship. However by (4) the larger the metacentric height the shorter is the period of roll, and the more uncomfortable is the ship; therefore choice of μ is an important feature of ship design.

What is at first surprising is how small μ can be compared with the size of the ship : for example a liner 300 metres long may have a metacentric height of only half a metre. Therefore we shall digress briefly to make some very rough estimates of μ and T, in order to give a quantitative feel for the problem complementary to the qualitative feel given by the subsequent catastrophe theory. We shall see in Section 7 that if G is too near M small alterations in the position of G may seriously increase the danger of capsizing.

Let $2a$ = beam of ship = width at water line,

A = area below water-line,

(x,y) = coordinates of B_θ relative to B_0,

$\rho = B_0M$ = radius curvature of $\mathfrak{B}$ at B_0.

Lemma 2. $\rho = \frac{2a^3}{3A}$.

Proof. Let $t = \tan\theta$.

Let 0^n denote order t^n.

Each wedge has area $\frac{1}{2}a^2t + 0^2$, and the coordinates of the centres of gravity of the wedges relative to the mid point of the water line are :

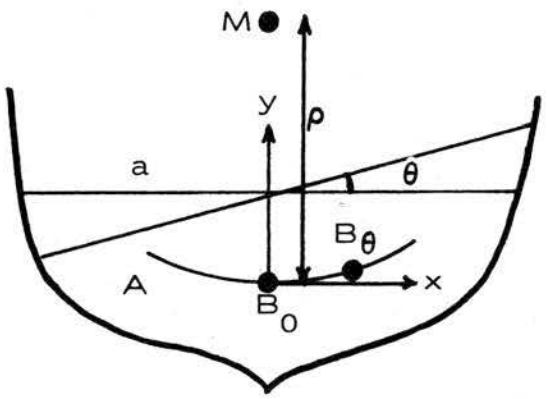

Figure 2. Computing ρ.

$$(\pm\frac{2a}{3} + 0^1, \pm\frac{at}{3} + 0^2).$$

The coordinates (x,y) of B_θ are given by taking moments of the wedges about B_0 :

$$Ax = (\tfrac{1}{2}a^2t)\frac{4a}{3} + 0^2 = \frac{2a^3t}{3} + 0^2$$

$$Ay = (\tfrac{1}{2}a^2t)\frac{2at}{3} + 0^3 = \frac{a^3t^2}{3} + 0^3$$

Therefore putting $\rho = \frac{2a^3}{3A}$, $x = \rho t + 0^2$

$$y = \tfrac{1}{2}\rho t^2 + 0^3 .$$

Therefore the equation of $\mathfrak{B}$ is

$$y = \frac{x^2}{2\rho} + 0(x^3),$$

which has radius of curve ρ at the origin, as required.

Define a ship to be wall-sided if the sides are parallel at the water-line, as in Figure 1. Let β denote the maximum angle of heel for which the water-line still meets the parallel part of the sides (in Figures 1 and 3, θ is about 25°).

Lemma 3. In a wall-sided ship the buoyancy locus for $|\theta| < \beta$ is precisely the parabola $x^2 = 2\rho y$.

Proof. In the proof of Lemma 2, leave out all the 0^n's.

In order to estimate the metacentric height and period of roll we now make a couple of very rough quantitative assumptions. Assume (i) that A is approximately a rectangle with the draught equal to a third of the beam, as in Figure 3. Therefore

$$A = 2a \times \frac{2a}{3} = \frac{4a^2}{3}$$

$$B_0M = \rho = \frac{2a^3}{3A} \text{ (by Lemma 2)}$$

$$= \frac{a}{2}.$$

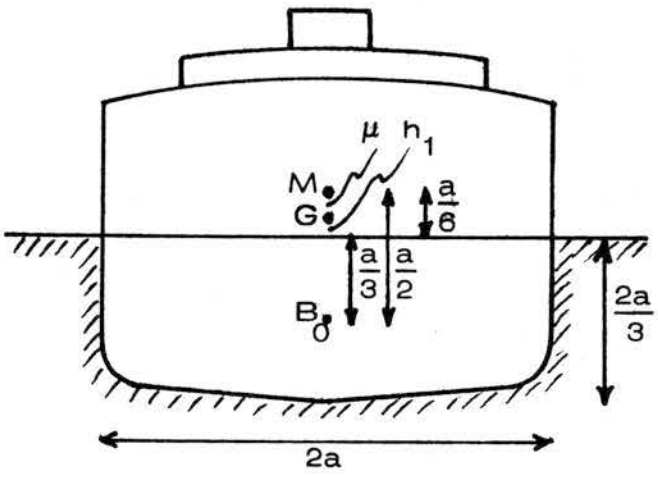

Figure 3. Estimate of μ.

Meanwhile B_0 is $\frac{a}{3}$ below the water-line, and so M is $\frac{a}{6}$ above. Therefore if h_1 = height of G above the water-line,

$$\mu = \frac{a}{6} - h_1 \quad \ldots\ldots\ldots\ldots\ldots\ldots (6)$$

Assume (ii) that the moment of inertia I is the same as that of a solid disk of radius a :

$$I = \frac{W}{g}\frac{a^2}{2} \quad \ldots\ldots\ldots\ldots\ldots\ldots (7)$$

where g = gravitational acceleration = 9.81 m/sec^2. We can now compute the period of roll:

$$T = 2\pi\sqrt{\frac{I}{W\mu}} \text{ by (4)}$$

$$= 2\pi\sqrt{\frac{a^2}{2g\mu}} \text{ by (7)}$$

$$= 1.42\,\frac{a}{\sqrt{\mu}} \quad \ldots\ldots\ldots\ldots\ldots\ldots \quad (8)$$

Although the above assumptions are crude the resulting orders of magnitude are not unreasonable for both naval and merchant ships [2 pages 107,335]. Where ships tend to differ is in the height of G above the water-line, and so let us work out a couple of examples of a destroyer and a liner in order to illustrate the contrast. In each case we assume typical values for the beam and position of G, and deduce the resulting metacentric height and period of roll.

Table 1		Destroyer	Liner
Assume	Beam, 2a	10m	30m
	Height of G above water-line, h_1	0	2m
Deduce	Metacentric height, μ, by (6)	0.8m	0.5m
	Period of roll, T, by (8)	8 secs	30 secs

Notice that the greater metacentric height of the destroyer gives a greater righting couple, and hence makes her more stable, so that she can perform tighter manoeuvres, as well as causing a faster roll. By contrast the lesser metacentric height of the liner makes her less stable, although this does not matter so much since she does not have to indulge in manoeuvres; meanwhile she benefits from the increased comfort of the slower roll and smaller accelerations, which ensure that the passengers are less likely to be seasick.

4. ROLLING IN A SEAWAY.

The forced oscillations induced by periodic waves, and the resonance that occurs when the period of the waves coincides with

the natural period T of rolling, were first studied by Bernoulli [3] in 1759.

Typical Atlantic ocean waves usually have a wave-length between 50 and 100 metres [2, page 177]. In deep water the wave-length determines both the speed and the period of the wave. For example a 60 metre wave has a speed of 35 Km/hour (= 19 knots) and a period of 6 seconds. The height of the wave from trough to crest is independent of the wave-length, and in the Atlantic, for instance, wave heights of over 6m occur on an average of 55 days in the year. In a 60m wave of height 6m the maximum inclination of water surface to the horizontal is approximately 18°.

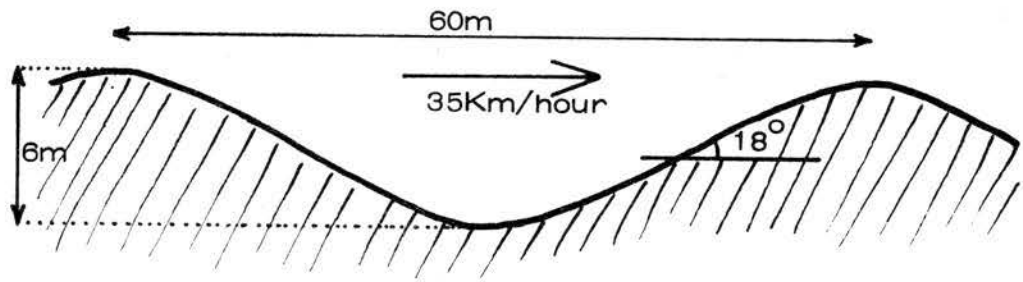

Figure 4. Typical Atlantic wave of period 6 seconds.

What is the effect of the waves on the ship? Suppose that in our 2-dimensional example the water surface is inclined at an angle α to the horizontal, as in Figure 5. The buoyancy force is the sum of all the pressures on the hull that would have sufficed to keep the displaced water in equilibrium with its surface inclined at angle α; hence the buoyancy force acts at $B_{\theta+\alpha}$ perpendicular to the water surface, in other words through M (approximately). Therefore the equation (2) for rolling must be modified to

$$I\ddot{\theta} = -W\mu(\theta+\alpha) \quad \ldots\ldots\ldots\ldots\ldots \quad (9)$$

Suppose now that we have a beam sea, in other words waves are coming from the side with period τ and maximum inclination α_o to the horizontal. The inclination α will be a periodic function of time, t, approximately equal to

$$\alpha = \alpha_o \cos \frac{2\pi t}{\tau} \quad \ldots\ldots\ldots\ldots \quad (10)$$

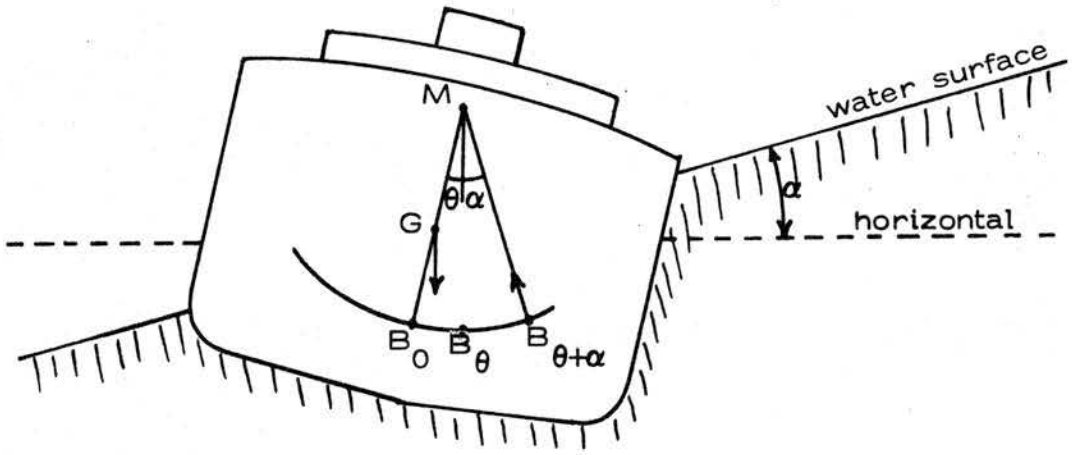

Figure 5. Inclined water surface.

Substituting (4) and (10) in (9) we obtain

$$\left(\frac{T}{2\pi}\right)^2 \ddot{\theta} + \theta = -\alpha = -\alpha_o \cos\frac{2\pi t}{\tau} . \quad \ldots\ldots (11)$$

The particular integral of (11) of period τ will give the rolling induced by the waves. The general solution of (11) will in fact be the sum of this particular integral together with a natural roll (3) of period T; however if we were to add a damping factor as in (5), then the latter would decay exponentially leaving only the particular integral, which is therefore an attractor of the dynamic. The particular integral will in fact be an amplification of the wave

$$\theta = \lambda\alpha = \lambda\alpha_o \cos\frac{2\pi t}{\tau} . \quad \ldots\ldots\ldots (12)$$

where λ is a constant amplifying factor. We can compute λ by substituting (12) into (11) :

$$\left[-\left(\frac{T}{\tau}\right)^2 + 1\right]\lambda\alpha = -\alpha .$$

Therefore $$\lambda = \left[\left(\frac{T}{\tau}\right)^2 - 1\right]^{-1} \quad \ldots\ldots\ldots\ldots (13)$$

We can now compute the effect of a typical Atlantic beam sea upon our destroyer and liner. Assume τ = 6 secs and $\alpha = 18^o$ as in Figure 4.

Table 2	Destroyer	Liner
Period of roll T, by Table 1	8 secs	30 secs
Amplifying factor λ, by (13)	$\frac{9}{7}$	$\frac{1}{24}$
Amplitude of induced roll, by (12)	23°	1°

Thus while the destroyer will be wallowing in the seaway the liner will hardly notice it. As Barnaby observes [2 p.337].

> "This is the great paradox of naval architecture - that the more stable the vessel really is, the more unstable she appears in a seaway."

He reinforces his observation with a revealing anecdote [2 p.355] that gives life to our computations :

> "This can be illustrated by the case of two yachts that were virtual sister ships, differing only in metacentric height. The captain of the first yacht reported her to be a magnificent sea-boat, extremely dry, and "stiff as a church" in a sudden squall [like our destroyer]. Her owner thought she was much too quick and lively in a seaway. As yachts have to be built for owners rather than for captains, the second vessel was given less metacentric height [like our liner]. The same captain transferred to the new yacht, and, in accordance with the best seafaring tradition, greatly preferred his old ship. His new command was wetter and more sluggish in a seaway, and, for these reasons, he considered her a worse sea-boat. The new owner was delighted, and said his yacht was "stiff as a church" in a seaway."

5. RESONANCE.

Before leaving the seaway we make some remarks concerning resonance. Suppose as before that the ship encounters waves of fixed period.

(i) If the wave-period, τ, happens to coincide with the natural roll-period, T, then the amplifying factor reaches a

maximum. Because of damping this maximum is finite. Formula (13) gives $\lambda = \infty$, but this is wrong because damping has been ignored. If, as in (5), a damping term of $2\varepsilon\dot{\theta}$ is added to (9), then for $\tau = T$ the resonant solution has a $\frac{\pi}{2}$ -phase-shift,

$$\theta = -\lambda\alpha_o \sin\frac{2\pi t}{T}$$

with amplifying factor $\lambda = \frac{\pi}{\varepsilon T}$. However the induced roll in this case may be so large that the linear theory is no longer valid. Indeed in heavy seas resonance may cause capsizing.

(ii) Let V, v denote the speeds of ship and wave. If the ship's course is such as to cause resonance we call it a sensitive course.

Lemma 4. If $V > v(1+\frac{\tau}{T})$ there are 4 sensitive courses.

Proof. Figure 6 shows how the period with which the ship encounters the waves depends upon the course. The blob represents the velocity of the waves, and the circle represents the different courses of the ship at speed V. The dashed line indicates the two courses perpendicular to the velocity of the waves (beam sea with period τ). The dotted lines indicate the two courses on which the ship will ride with the waves (period ∞). The other four lines indicate the sensitive courses. In order to encounter the waves with period T, the relative velocity of the ship must have a component $\pm \frac{v\tau}{T}$ in the direction of the waves. Therefore the ship's velocity is $v(1\pm\frac{\tau}{T})$ in this direction. The condition for the four

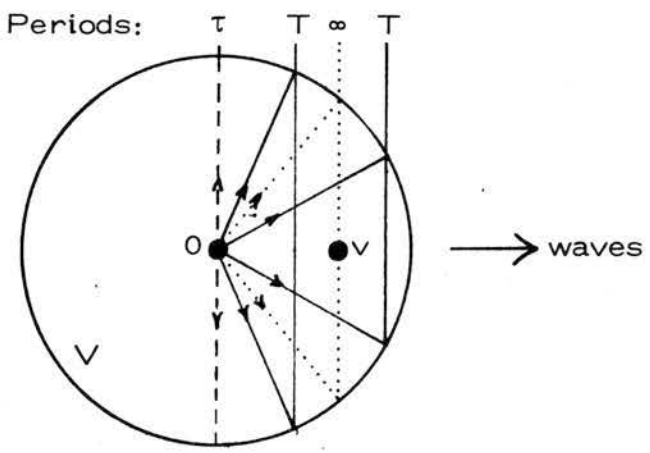

Figure 6. Sensitive courses.

directions to exist is that this component be less than V. This completes the proof. On the two sensitive courses closest to the wave direction the ship overtakes the waves, while on the other two ship is overtaken by the waves.

(iii) The non-linearity of the accurate rolling equation makes a wall-sided ship behave like a hard spring for small angles of roll, and a soft spring for large angles of roll (see Section 9 and Figure 19 below). The latter is liable to produce a Duffing effect [8,15] near resonance, as shown in Figure 7. If there is a Duffing effect, then when the ship reduces speed on a sensitive course overtaking the waves the amplitude of induced roll may at first increase slightly, and then drop suddenly when a critical speed V_1 is reached. Conversely, if the ship increases speed again a hysteresis delay will occur, during which the roll will remain deceptively small, until a higher critical speed V_2 is reached,

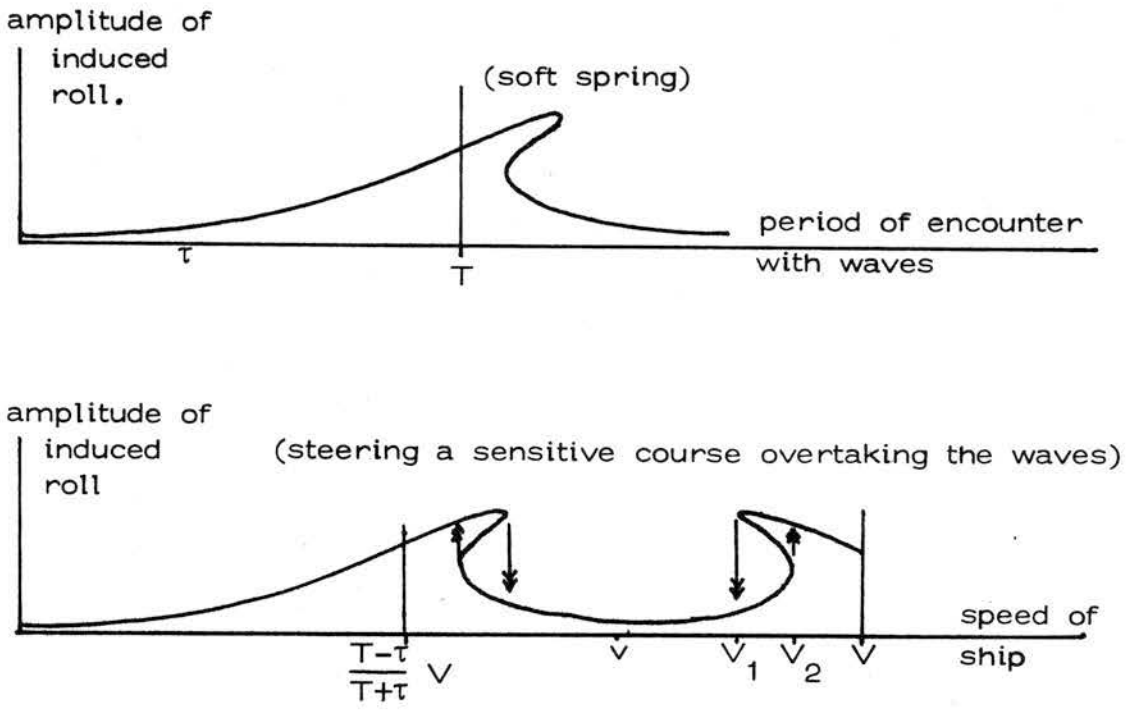

Figure 7. Duffing effects.

when the amplitude will suddenly increase again. Such a catastrophic jump could be dangerous because the dynamic stability of the resulting resonance might lead to capsizing before remedial action had time to take effect. Similar catastrophes occur near $(\frac{T-\tau}{T+\tau})V$, which in the case of the liner above equals $\frac{3}{5}V$. Note these catastrophes are different from those in the main model in Sections 7 - 14 below.

6. PITCHING AND HEAVING.

Passing from the 2-dimensional problem to the 3-dimensional problem, the buoyancy locus $\mathfrak{B}$ becomes a convex closed surface rather than a convex closed curve. Therefore $\mathfrak{B}$ has two principle directions of curvature at B_0, and two centres of curvature. One is the metacentre M for rolling about the longitudinal axis that we have already discussed, and the other is the metacentre M^* for pitching about the transverse axis. We now estimate the period of pitching, using the same notation as before, only with asterisks.

For simplicity assume (i) that the area below water is a rectangle with length L and draught D. Then by Lemma 2 the radius of curvature is

$$\rho^* = \frac{2(L/2)^3}{3LD} = \frac{L^2}{12D} .$$

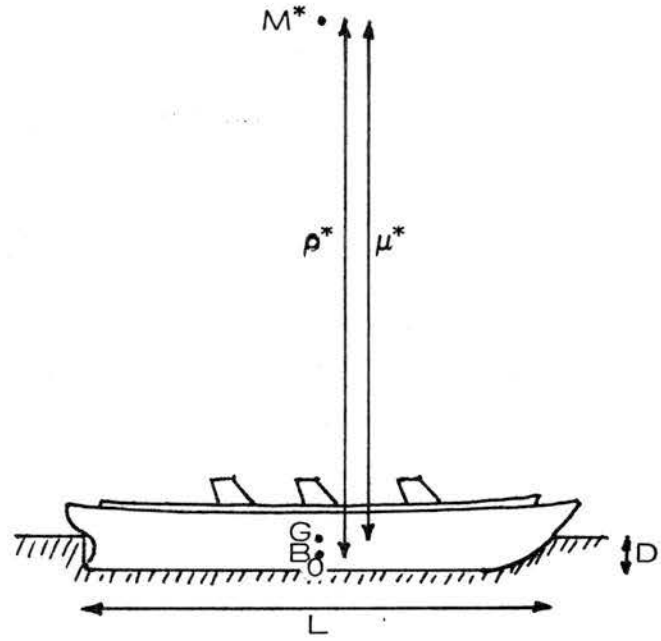

Figure 8. Pitching metacentre.

Assuming (ii) that $L > 24D$, then $\rho^* > 2L \gg B_0G$, and therefore B_0G can be ignored in the estimate of μ^* :

$$\mu^* = \rho^* = \frac{L^2}{12D} \quad \ldots\ldots\ldots\ldots\ldots (14)$$

Assume (iii) that the moment of inertia about the transverse axis is the same as that of a rod of length L. Therefore

$$I^* = \frac{W}{g}\frac{(L/2)^2}{3} = \frac{WL^2}{12g} \quad \ldots\ldots\ldots (15)$$

By (4) the period of pitching is

$$T^* = 2\pi\sqrt{\frac{I^*}{W\mu^*}}$$

$$= 2\pi\sqrt{\frac{D}{g}} \quad \text{by(14) and (15)} \quad \ldots\ldots (16)$$

$$= 2\sqrt{D}, \text{ approximately.}$$

Applying this to our two ships :

		Destroyer	Liner
Assume	Length, L	100m	300m
	Draught, D	3.3m	10m
Deduce	Pitching metcentric height μ^*, by (14)	250m	750m
	Period of pitching T^*, by (16)	4 secs	6 secs

Since μ^* is several hundred times larger than μ, the ship is far more stable with respect to pitching than to rolling, and hence the period is short, and amplitude kept small. The accelerations involved may be greater, and hence pitching is sometimes more uncomfortable than rolling.

Heaving refers to oscillations up and down. Let q denote the height of the ship above the equilibrium position. For a wall-sided ship of draught D, the volume of displaced water is reduced by a factor of approximately $\frac{q}{D}$.

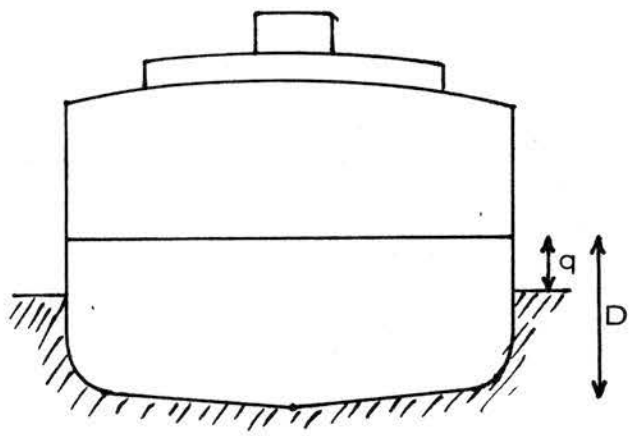

Figure 9. Heaving.

Therefore the buoyancy force is reduced by the same factor, and so there is a net downward restoring force of $\frac{Wq}{D}$. Therefore by Newton's law

$$\frac{W}{g}\ddot{q} = -\frac{Wq}{D} .$$

Therefore $$\ddot{q} = -\frac{g}{D}q \quad \ldots\ldots\ldots\ldots\ldots\ldots \quad (17)$$

Hence the period for heaving is the same as that for pitching (16). In practice of course the periods differ slightly, because our assumptions are too imprecise. However the proximity of the periods implies that pitching and heaving will be coupled, and the classical theory of the coupling originated with Krilov in 1893 (see [3]).

The other 3 normal modes of oscillation, yawing (about the vertical axis), swaying (from side to side) and surging (fore and aft) differ from rolling, pitching and heaving in that buoyancy does not provide a natural restoring force; therefore these modes tend to occur only as induced, or secondary effects. We express the difference in group-theoretic terms in Lemma 12 below. This completes our elementary sketch of the classical linear theory, and we now begin the catastrophe theory, which is the main business of the paper.

7. CUSP CATASTROPHE AT THE METACENTRE.

For simplicity return to the 2-dimensional problem of rolling. For large angles the linear theory is no longer valid because the buoyancy force no longer goes through M. We need to look at not just one centre of curvature, but all of them. Therefore define the <u>metacentric locus</u> $\mathfrak{M}$ of the ship to be the locus of centres of curvature of the buoyancy locus $\mathfrak{B}$, in other words $\mathfrak{M}$ is the evolute of $\mathfrak{B}$.

Now B_0 is a point of symmetry of $\mathfrak{B}$ where the radius of curvature is stationary, and hence M is a cusp point of $\mathfrak{M}$. The

geometric question arises : Which way does the cusp branch, upwards or downwards? In Figure 10 we show two cases arising from different shapes of hull, on the left a modern wall sided ship, and on the right an old-fashioned canoe, shaped like an ellipse with major axis horizontal.

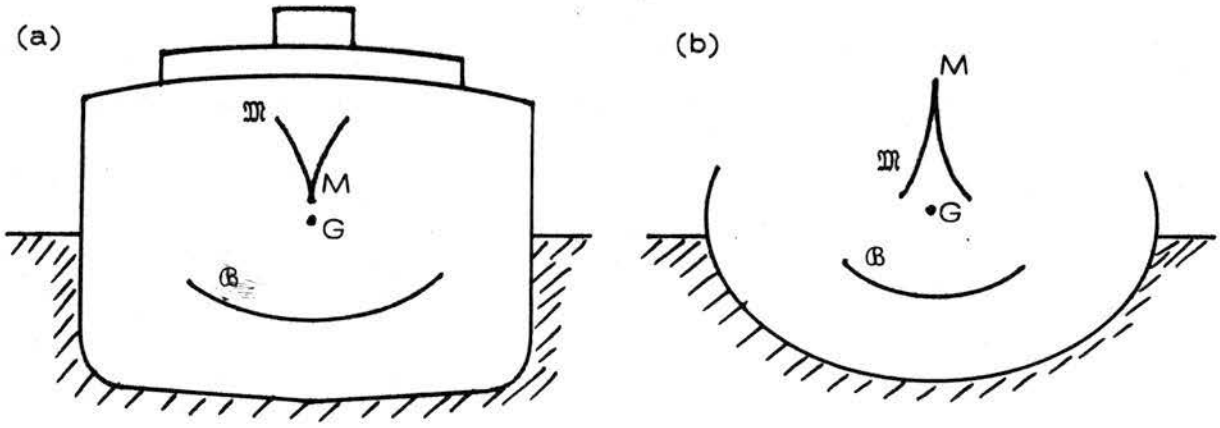

Figure 10. Cusps in ship (a) and canoe (b).

Lemma 5. The cusp branches upwards in the ship (a) and downwards in the canoe (b).

Proof. In a wall-sided ship $\mathcal{B}$ is locally a parabola $x^2 = 2\rho y$, by Lemma 3. This has evolute

$$27\rho x^2 = 8(y-\rho)^3 ,$$

which is a cusp branching upwards. The result for an elliptical-shaped hull follows from the Corollary to Lemma 7 below.

We will now explain the physical significance of which way the cusp branches. Suppose that the position of the centre of gravity of the ship changes for some reason : for example the canoeist might lean over the side, or stand up, or put up a mast. In a liner the passengers might crowd to one side to see something interesting. A cargo boat might load or unload, or restow its cargo (see Figures 27 and 28 below). In heavy weather the cargo might shift* by itself, or slosh about if liquid, or the ship might

---

* Capsizing and the shifting of cargo are still hazards. During 1975 according to Lloyds Casualty Return [10] 125 merchant ships foundered mostly in heavy weather (not to mention another 211 lost, missing, burnt, wrecked, or in collison). Of the 125 foundered 13 are known to have capsized and sunk, 14 others developed a list before sinking, and in 9 cases the list was known to be due to the cargo shifting.

accumulate ice to windward, or sea-water on deck. Fishing vessels may be tempted by a good catch to take on more than is advisable. For simplicity assume for the moment that the position of G changes without altering the total weight, so that the buoyancy locus remains the same (in Section 14 we allow for change of weight).

Question : given the position of G, at what angles can the ship float in equilibrium?

Answer : by Lemma 1 it will be those angles θ, such that G lies on the normal N_θ to $\mathcal{B}$ at B_θ. But the normals to $\mathcal{B}$ are tangents to $\mathcal{M}$; therefore the angles are obtained by drawing tangents from G to the cusp.

In Figure 11 we plot the graph of θ as a function of G, for the two boats pictured in Figure 10. In each case the position of G is represented by a point in the horizontal plane, C. The value of θ is represented by a point on the vertical axis $\mathbb{R}$, and for simplicity we assume $|\theta| < \beta$, where β is some suitable bound (in the full model in Section 10 below, we allow θ to be arbitrary). On the vertical line above each position of G we plot the corresponding equilibrium values of θ, and as G varies these points trace out a smooth surface, which we call the equilibrium surface, E. We shall prove in Theorem 2 below that in each case E is a cusp-catastrophe. By definition

$$E = \{(G,\theta);\ G \in N_\theta,\ |\theta| < \beta\}$$
$$= \{N_\theta \times \theta;\ |\theta| < \beta\},\ \subset C \times \mathbb{R}\ .$$

Therefore E is a smooth ruled surface, consisting of horizontal lines parallel to the normals, one for each θ. In other words E is the normal bundle of $\mathcal{B}$. Over the outside of the cusp E is single-sheeted because if G lies outside (as in Figure 11(a)) there is only one tangent from G to the cusp. On the other hand over the inside of the cusp E is triple-sheeted, because if G lies inside (as in Figure 11(b)), there are three tangents from G to the cusp.

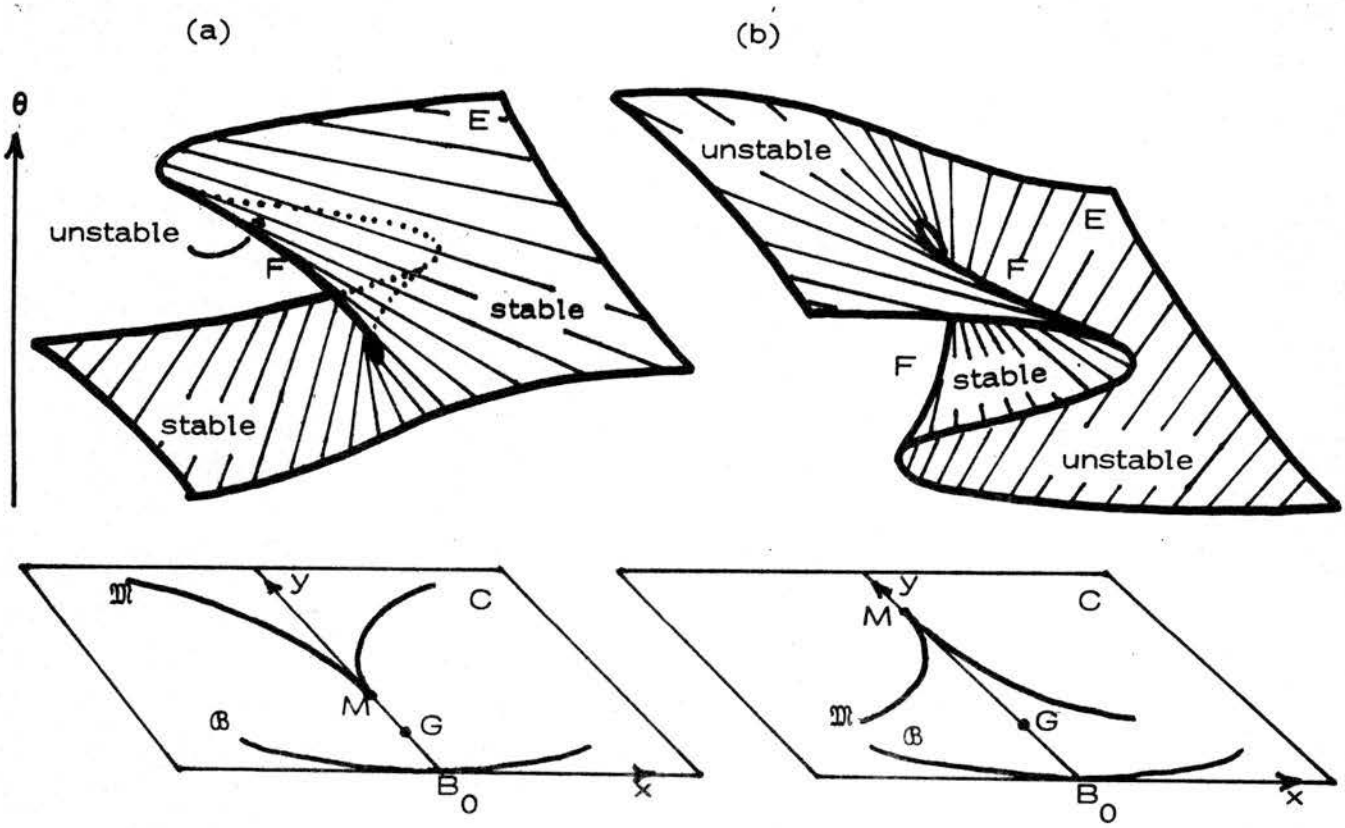

Figure 11. The cusp-catastrophe in the ship (a) and the canoe (b).

If E is projected down onto C it becomes folded along a curve, called the fold curve F, which projects onto the cusp. Hence the cusp is a bifurcation set. F separates E into two components, one representing stable equilibria and the other unstable equilibria. For example if G lies on the axis of symmetry (the y-axis) then by equation (2) in Section 1 the equilibrium position $\theta = 0$ is stable or unstable according as to whether the metacentric height μ is positive or negative, in other words whether G is below or above M.

If, further, G lies inside the cusp then the $\theta = 0$ equilibrium is represented by a point on the middle sheet of E, whilst the other two equilibria are represented by points on the upper and lower sheets of E. We call these heeling angles if the cusp branches upwards, as in case (a), and capsizing angles if the cusp branches downwards, as in case (b).

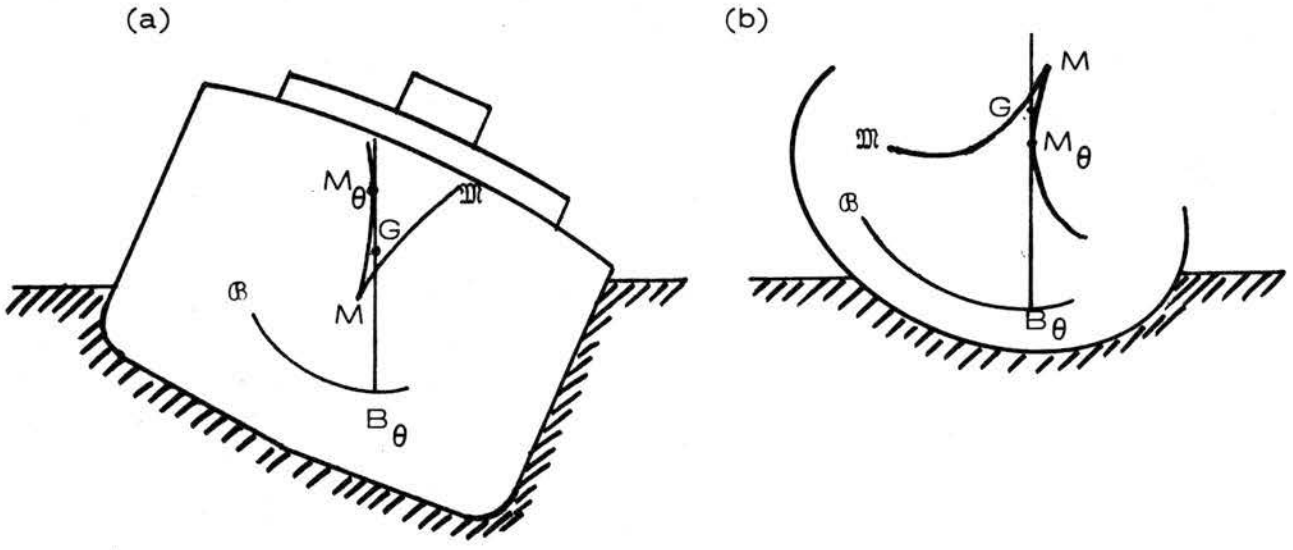

Figure 12 (a) Heeling angle. (b) Capsizing angle.

Here the difference between the two boats becomes apparent because :

Lemma 6. Heeling angles are stable, whereas capsizing angles are unstable.

Proof. Let θ be a heeling or capsizing angle. If M_θ denotes the corresponding metacentre, the centre of curvature of $\mathfrak{B}$ at B_θ, then the tangent from G touches the cusp at M_θ. Figure 12 shows that in case (a) G lies below M_θ, and so the ship behaves stably like a pendulum hanging from M_θ. By contrast in case (b) G lies above M_θ, and so the canoe behaves unstably, balanced precariously over M_θ; any perturbation reducing θ will produce a righting couple that returns the canoe upright, whereas any perturbation the opposite

way will produce an opposite couple, that will cause the canoe to turn turtle.

Therefore in Figure 11(a) the upper and lower sheets of E are stable, while the middle sheet over the inside of the cusp is unstable. In Figure 11(b) it is the other way round, and so in this case E is called a dual cusp-catastrophe. The difference is emphasised in Figure 13 which shows in each case the section of E over the y-axis, rotated through 90° so as to make the y-axis vertical. The section in each case consists of the line $\theta = 0$ bisecting a curve (which is a parabola modulo θ^4). The stable equilibria are shown firm, and the unstable dotted. In case (a) the curve is stable and rising and represents heeling angles, while in case (b) it is unstable and falling and represents capsizing angles. The specific angles are given by the intersection of the curve with the horizontal line through G.

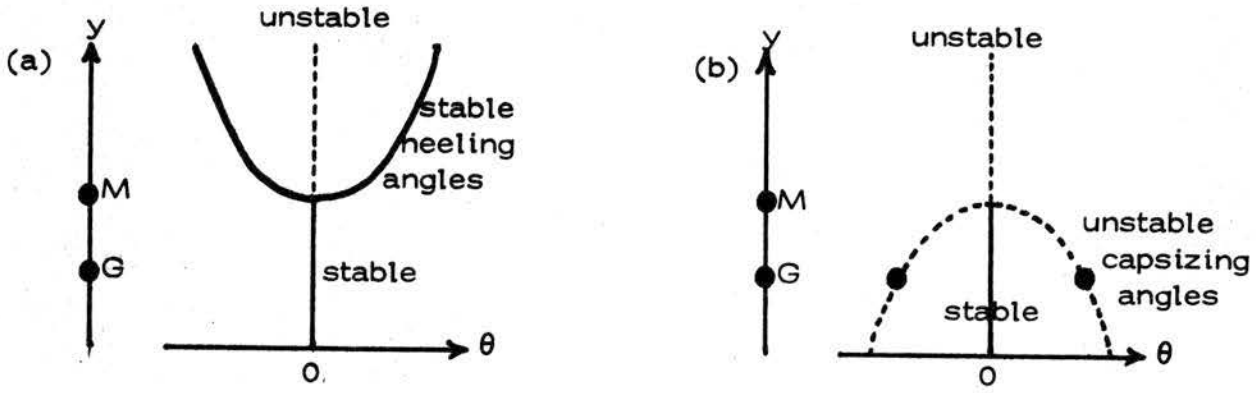

Figure 13. Sections of E over the y-axis for (a) ship and (b) canoe.

Now imagine an experiment in which the centre of gravity is raised up the y-axis past M. In case (a) when G passes M the ship will heel over to one side or the other, and will settle into stable equilibrium at the heeling angle. This happens for instance in certain old cargo boats when they unload, because they used to be designed with negative metacentric height when empty (see

[2, p.71] and Figures 27, 28 below). It also tends to happen in toys like model gondolas for the same reason, and sometimes the heel can be corrected by loading the model with a little ballast.

Suppose that G is on the y-axis above M with the ship heeled to the right, represented by a point on the upper sheet of Figure 11(a). If G is now moved to the left the ship will stay heeled to the right until G crosses the left side of the cusp, when it will suddenly heel over to the left; this is represented in Figure 11(a) by the point crossing the fold curve and jumping catastrophically onto the lower sheet. Conversely if G is now moved to the right then the ship will delay until G crosses the right side of the cusp when it will suddenly heel back again. Therefore in case (a) the cusp is a heeling bifurcation set.

By contrast case (b) is more dangerous because if G is raised up the y-axis past M the canoe will suddenly capsize. Worse still, if G happens to be off-centre when it is raised then it will cross the cusp sooner because the cusp branches downwards, and hence capsize sooner. This imperfection-sensitivity explains why when standing up in a canoe it is advisable to keep perfectly in the centre. Similarly if G is moved sideways, then as soon as G crosses either side of the cusp the canoe will capsize. A graphic description of such an event is given by Gerald Durrell [6, p.163].

> "Peter nodded, braced himself, clasped the mast firmly in both hands, and plunged it into the socket. Then he stood back, dusted his hands, and the Bootle-Bumtrinket, with a speed remarkable for a craft of her circumference, turned turtle."

Evidently raising the mast raised G close to the metacentre where the cusp was very narrow, and stepping back was sufficient to cause G to cross the cusp - or maybe only just to reach the cusp, and it was actually the dusting of the hands that gave the final perturbation across it. Durrell goes on to explain how the problem was solved :

> "For the rest of the morning he kept sawing

bits off the mast until she eventually floated upright, but by then the mast was only about three feet high."

Summarising :

Theorem 1. An upward branching cusp is a heeling bifurcation set, and a downward branching cusp is a capsizing bifurcation set.

Notice that this theorem only refers to the statics, because although we have used local righting couples to determine the local nature of the stability, the global dynamics has been ignored. We shall return to the dynamics again in Section 10.

8. GLOBAL METACENTRIC LOCUS.

We have yet to prove that the cusp in a canoe branches downwards. The easiest way to tackle this is to investigate the global metacentric locus of a completely elliptical ship, (like a submarine before it submerges).

Lemma 7. The buoyancy locus of an ellipse is a similar ellipse.

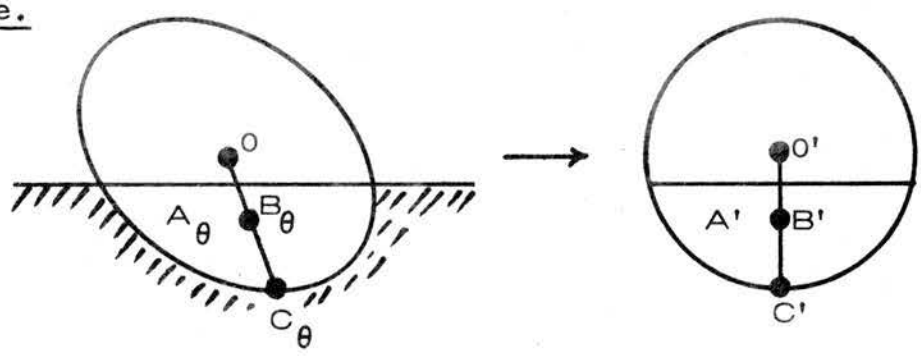

Figure 14.

Proof. Let O denote the centre of the ellipse, and C_θ the lowest point when heeled at angle θ. The line OC_θ bisects all horizontal chords, therefore bisects the region A_θ below the water line, and hence contains the centre of buoyancy B_θ. Map the ellipse onto a circle by an affine area-preserving map, and let A',B',C',O' denote the images of $A_\theta, B_\theta, C_\theta, O$. Then B' is the centre of gravity of A', and since the area of A' is independent of θ

The equation of E in (x,y,θ)-space is formally the same as that of the normal N_θ in (x,y)-space, with the proviso that θ is reinterpreted as a coordinate rather than a parameter. In case (a) of the wall-sided ship $\mathfrak{B}$ is locally a parabola

$$x^2 = 2\rho y,$$

by Lemma 3. The normal N_θ is given by

$$x + (y-\rho)\tan\theta - \frac{1}{2}\rho\tan^3\theta = 0.$$

As a surface this is differentially equivalent (in the sense of [13]) to

$$x + (y-\rho)\theta - \theta^3 = 0,$$

which is a canonical cusp catastrophe at $(0,\rho)$ with x,y as normal and splitting factors.

In case (b) of the canoe, $\mathfrak{B}$ is an ellipse by Lemma 7, and the equation of the ellipse with radius of curvature ρ at the origin and eccentricity e (where e is the ratio of the vertical axis to horizontal axis) is :

$$x^2 + \left(\frac{y}{e}\right)^2 = 2\rho y.$$

The normal N_θ is given by

$$x + (y-\rho)\tan\theta + \rho(1-e^2)\tan\theta\,[1-e(e^2+\tan^2\theta)^{-\frac{1}{2}}] = 0$$

Since $e < 1$, this is differentially equivalent, as a surface, to

$$x + (y-\rho)\theta + \theta^3 = 0,$$

which is a canonical cusp-catastrophe at $(0,\rho)$ with $-x,-y$ as normal and splitting factors. This completes the proof.

Remark. If in case (b) the eccentricity e is increased until $e > 1$, this converts the horizontal axis of the ellipse into the minor axis, and changes the sign of θ^3, converting the cusp from downwards branching into upwards branching, as in case (a).

The question now arises : what is the complete metacentric locus for a modern wall-sided ship? Where does $\mathfrak{M}$ go to after the initial upward branching of the cusp? How does $\mathfrak{M}$ compare globally with the 4-cusp evolute of an elliptical hull shown in Figure 15? We start by looking at a rectangle :

the ratio $O'B'/O'C' = \text{constant}$, k say, independent of θ. Since the map is affine $OB_\theta/OC_\theta = k$. Therefore, as C_θ traces out the ellipse, B_θ traces out a similar ellipse k times the size. This completes the proof. Notice that the result is independent of the weight (or density) of the ship.

Corollary. The metacentric locus of an ellipse has 4 cusps as shown in Figure 15.

For it is merely the evolute of the buoyancy locus, which by the lemma is a similar ellipse. In particular this completes the proof of Lemma 5, for in an elliptical shaped canoe with major axis horizontal, the metacentre M is the topmost cusp, and hence the cusp branches downwards.

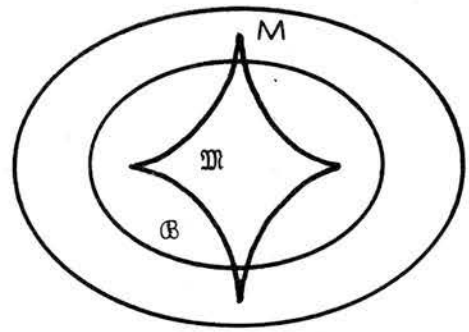

Figure 15.

Remark. In the 3-dimensional situation exactly the same proof shows that the buoyancy locus of an ellipsoid is a similar ellipsoid. The evolute of an ellipsoid, however, is more difficult to visualise because it consists of two sheets corresponding to the two metacentres, one for rolling and one for pitching. It can be regarded as 2 spheres, pinched along 3 elliptical cusped edges, one of which contains 4 hyperbolic umbilics [5].

Theorem 2. The equilibrium surface E has a cusp catastrophe at the metacentre M.

Proof. If the buoyancy locus $\mathfrak{C}$ is generic, then from general theory its evolute $\mathfrak{M}$ will have a generic cusp at M, and its normal bundle E will have a cusp catastrophe. However we cannot be sure that the curves in question are generic without checking the explicit formulae for wall-sided and elliptical ships.

Theorem 3. In a rectangular hull of density ½ the buoyancy locus is the union of 4 pieces of parabolas, and the metacentric locus has 8 cusps.

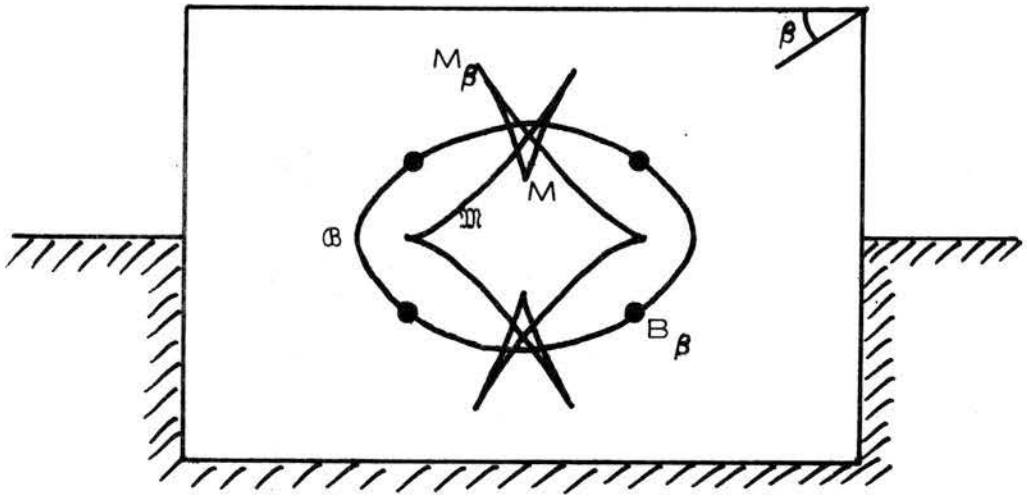

Figure 16. The metacentric locus of a rectangle.

Proof. The rectangle is a wall-sided ship for $|\theta| < \beta$, where β is the inclination of the diagonal to the horizontal. Therefore for $|\theta| < \beta$, $\mathfrak{B}$ is a piece of a parabola by Lemma 3, and contributes an upwards branching cusp to $\mathfrak{M}$ by Lemma 5. There are 4 pieces, corresponding to the 4 sides of the rectangle. Two pieces of $\mathfrak{B}$ join at B_β, and here the two parabolas have the same tangent by Lemma 1, the same radius of curvature by Lemma 2, and hence the same centre of curvature M_β. Therefore two pieces of $\mathfrak{M}$ touch at M_β, producing a parabolic cusp. Therefore $\mathfrak{M}$ is continuous, containing 4 generic cusps (of index $\frac{3}{2}$) separated by 4 non-generic parabolic cusps (of index 2), as shown in Figure 16.

Remark 1. If the density is reduced (or increased) the 4 parabolas in $\mathfrak{B}$ are separated by 4 pieces of rectangular hyperbolas. When the density reaches $\frac{1}{2}\tan\beta$ then 4 swallowtails appear giving raise to another 8 cusps in $\mathfrak{M}$, making 16 in all (see Figures 25 and 28 below).

Remark 2. The non-genericity of the 4 parabolic cusps is due to the non-smoothness of the corners of the rectangle. If the corners are rounded-off in a C^∞-fashion, then the 4 parabolic cusps become generic, and the qualitative shape of $\mathfrak{M}$ is stable under small perturbations. Now the cross-section of a large modern ship can be regarded as a perturbation of a rounded-off rectangle. Therefore :

Conjecture. Large modern ships have metacentric locus $\mathfrak{M}$ similar to that in Figure 16. Detailed computations for individual ships show the top three cusps [11, p.135].

Remark 3. The evolution of hull shape from ellipse to rounded rectangle will cause a bifurcation of $\mathfrak{M}$ from the 4 cusps in Figure 15 to the 8 cusps in Figure 16. The reader familar with the elementary catastrophes will recognise immediately canonical sections of the butterfly catastrophe [12].

Problem. Prove, for an explicit isotopy of hull shape, that the bifurcation is an unbiased butterfly, in other words is equivalent to the symmetry section of the butterfly catastrophe given by putting the bias factor (the coefficient of θ^3) equal to zero. The governing potential at the bifurcation point should be

$$-k\theta^6 + i\theta^4 + \frac{1}{2}(\rho - y)\theta^2 - x\theta,$$

where x,y are coordinates of G, ρ the radius of curvature, $k > 0$, and i the isotopy parameter running from $i < 0$ for the canoe to $i > 0$ for the ship. The unbias is due to the symmetry of the ship, and a full butterfly should be obtained by introducing a bias factor measuring lop-sidedness of hull.

Remark 4. Globally the bifuraction set of the modern ship is not so very different from that of a canoe, and therefore the ship is not so safe as Theorem 1 would at first sight suggest. Therefore it is necessary to take another qualitative look at the heeling and capsizing. We assume the ship has metacentric locus similar to Figure 16, as conjectured above.

Theorem 4. The only heeling part of the metacentric locus $\mathfrak{M}$ is the cusp at M, shown dotted in Figure 17(a); the rest is capsizing. The equilibrium surface E is a section of a dual* butterfly catastrophe, as shown in Figure 17(b). The stable equilibria are shown shaded. Therefore for stability G must lie below $\mathfrak{M}$.

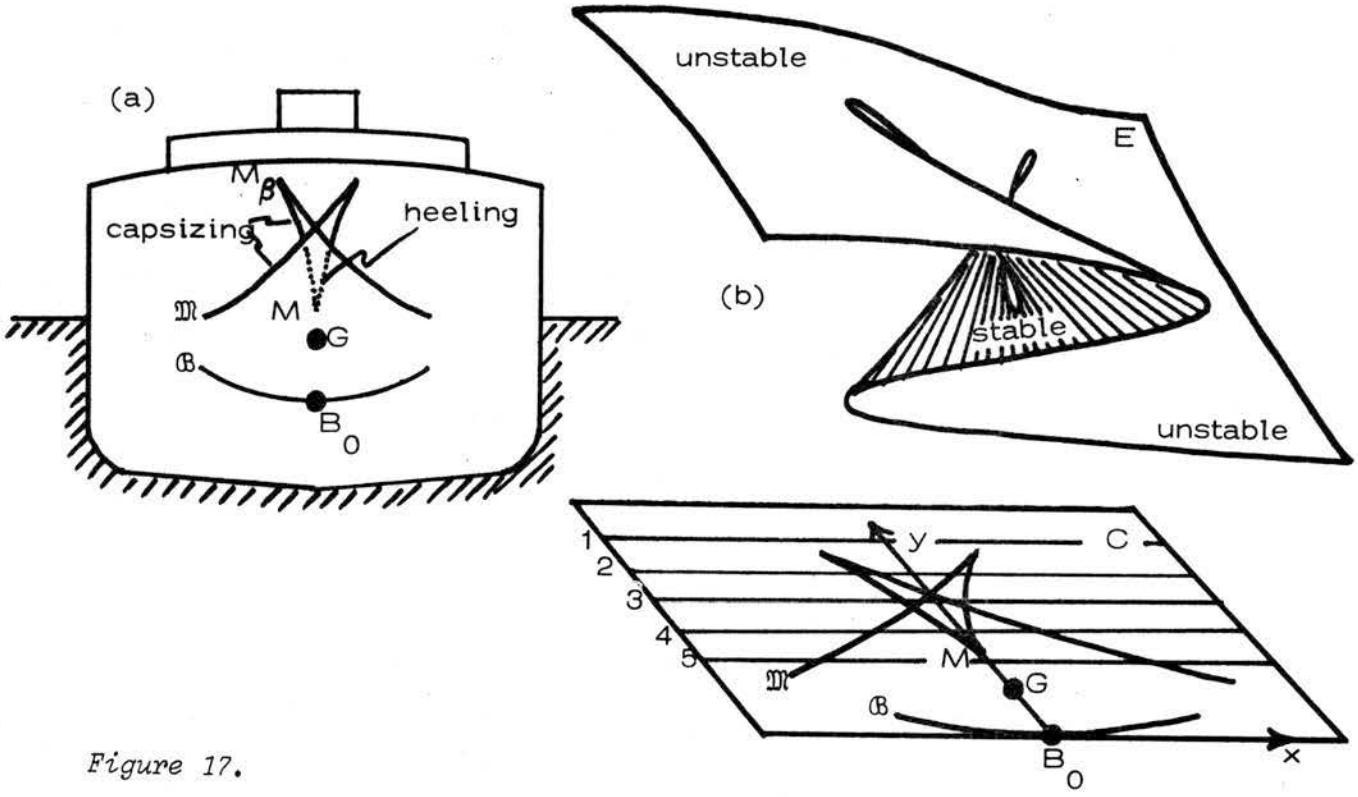

Figure 17.

(a) Metacentric locus $\mathfrak{M}$ is part heeling (dotted) and part capsizing (firm).

(b) Equilibrium surface E is a section of a butterfly catastrophe.

Proof. The bifurcation set in Figure 16 determines that E is a butterfly section, as shown in Figure 17(b) (see [12,13]). The identification of stable and unstable components of E is deduced from Figure 11(a), which is a subset of Figure 17(b). Hence E is a dual butterfly. The heeling and capsizing parts of $\mathfrak{M}$ are determined by consideration of the 5 sections of E over the 5 lines

* The dual butterfly [13] has germ $-\theta^6$, as opposed to the butterfly which has germ $+\theta^6$. This is the only application I know of the dual butterfly.

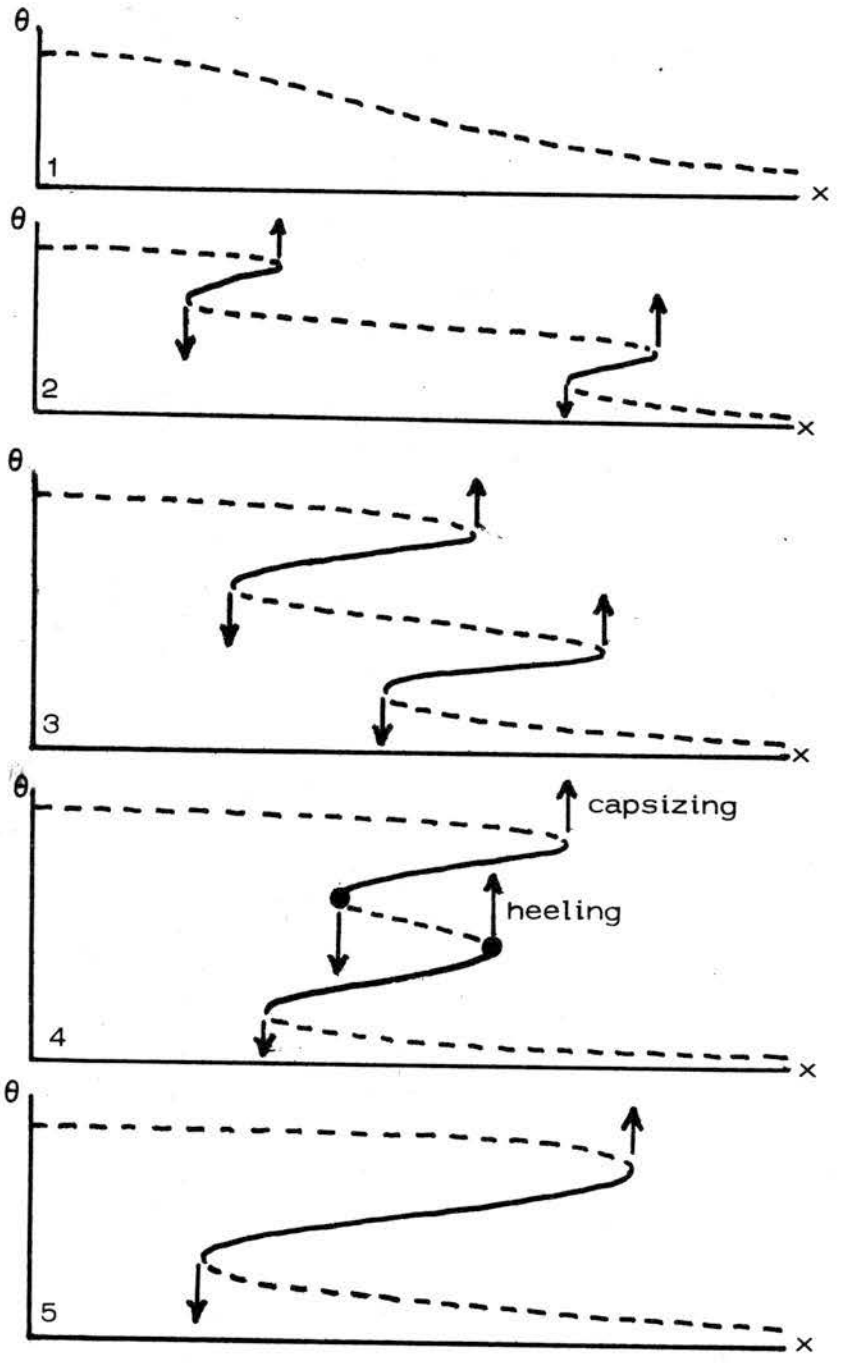

Figure 18. Sections of E.

parallel to the x-axis in Figure 17(b), as follows. The 5 sections are shown in Figure 18, with firm lines indicating stable equilibria, and dashed lines unstable equilibria. The nature of the stability determines which way the couple acts upon θ, and hence determines the direction of the catastrophic jump at each fold point, as indicated by the arrows. The catastrophe is heeling if the arrow

tip stands on another stable sheet, and this only occurs for the middle two arrows of the fourth section. Hence the roots of those arrows (indicated by blobs) are the only two heeling parts of $\mathfrak{M}$. All the other parts of $\mathfrak{M}$ induce capsizing catastrophes. This completes the proof of Theorem 4.

9. LEVER ARM CURVE.

Assume G fixed. Recall that ℓ denotes the lever arm of the righting couple (see Figure 1(b)). The graph of ℓ for $0 \leq \theta \leq \frac{\pi}{2}$ is called the lever arm curve, and is illustrated in Figure 19 for the two boats shown in Figure 10. The slope of the lever arm curve at the origin is equal to the metacentric height, μ, because for small θ the linear approximation of the lever arm is $\ell = \mu\theta$.

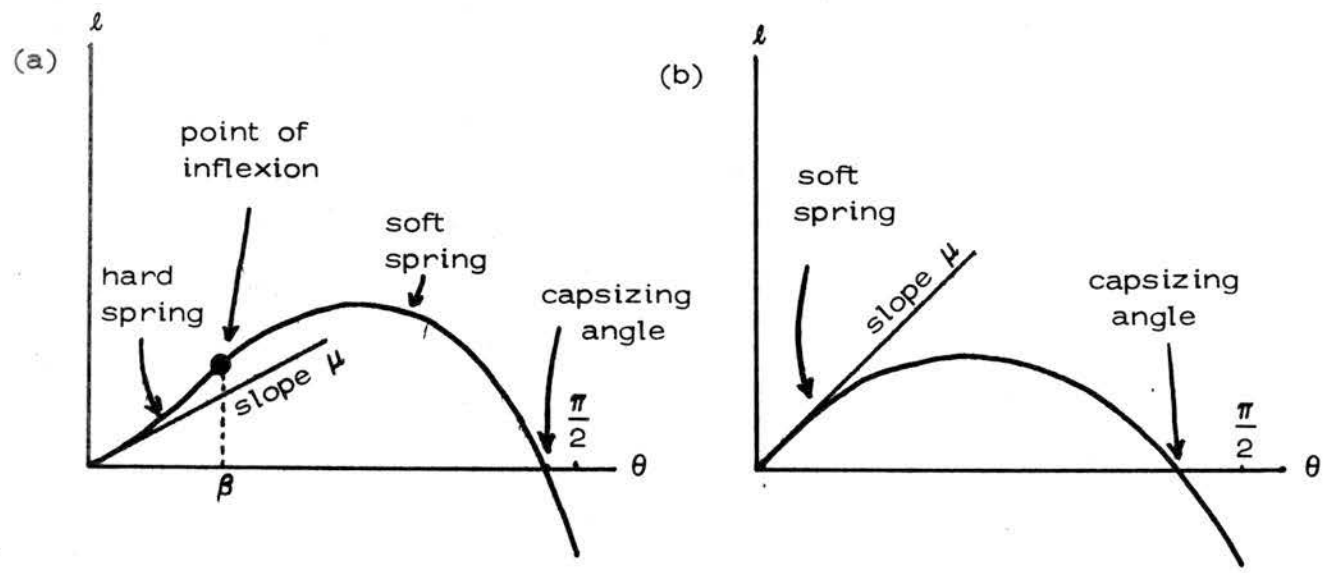

Figure 19. Lever arm curves for (a) ship and (b) canoe.

Lemma 8. In a wall-sided ship (a) the curvature of the lever arm curve is initially positive (like a hard spring), whereas in a canoe (b) it is negative (like a soft spring).

Proof. In the case of a wall-sided ship the normal N_θ is given by

$$x \cos\theta + (y-\rho)\sin\theta - \frac{1}{2}\rho \tan^2\theta \sin\theta = 0$$

by the proof of Theorem 2. Hence the distance ℓ from $G = (0, \rho-\mu)$ to N_θ, choosing the sign to be positive, is

$$\ell = \mu \sin\theta + \frac{1}{2}\rho \tan^2\theta \sin\theta$$

$$= \mu\theta + (\frac{\rho}{2} - \frac{\mu}{6})\theta^3 + O(\theta^5) .$$

Since $\mu < \rho$ the coefficient of θ^3 is positive, and hence for θ positive and small, the curvature is positive. In the canoe the normal N_θ is given by

$$x \cos\theta + (y-\rho)\sin\theta + \rho(1-e^2)\sin\theta[1-e(e^2+\tan^2\theta)^{-\frac{1}{2}}] = 0 .$$

Hence

$$\ell = \mu \sin\theta - \rho(1-e^2)\sin\theta[1-e(e^2+\tan^2\theta)^{-\frac{1}{2}}]$$

$$= \mu\theta - \theta^3[\frac{\rho}{2} e^{-2}(1-e^2) + \frac{\mu}{6}] + O(\theta^5) .$$

Since $e < 1$ the coefficient of θ^3 is negative, and hence, for θ small and positive, the curvature is negative.

Remark 1. In Figure 19 the difference in sign between the initial curvatures can be intuitively explained by which way the cusps branch in Figure 10. For in case (a) the upward branching causes the hard spring, while in case (b) the downward branching causes the soft spring. To be precise the conditions are slightly different : the cusp branches up or down as $e \gtrless 1$, whereas the curvature is hard or soft as $e \gtrless (1-\mu/3\rho)^{-\frac{1}{2}}$, and since $\mu < \rho$ this constant lies between 1 and $\sqrt{3/2}$.

Remark 2. In Figure 19(a) the change of curvature from hard to soft at the point of inflexion can be intuitively explained by the butterfly section in Figure 16. In the case of a rectangular

hull, the initial hard spring is caused by the upward branch MM_β of $\mathfrak{M}$, the point of inflexion occurs at the angle β of the cusp M_β, and the subsequent soft spring is caused by the subsequent downward branch of $\mathfrak{M}$, to the capsizing angle, as indicated in Figure 12(b). In the wall-sided ship Figure 17 the same holds, except that the smoothness of hull causes the angle at which the inflexion occurs to be displaced slightly below that at which the cusp occurs.

Remark 3. The dynamical importance of the lever arm curve was first recognised by Atwood in 1796. Its use for judging stability in the design of ships was first proposed by Reed in 1868, and today various key features of the curve are widely used as stability criteria by naval architects and marine authorities [9]. What is new in this paper is the relationship between seemingly ad hoc features of the curve and generic properties of the metacentric locus arising from canonical sections of the butterfly catastrophe.

10. CATASTROPHE MODEL FOR ROLLING.

In Sections 2 - 6 we have discussed the local linear dynamics, and in Sections 7 - 9 the non-linear statics. We now weld the two together in order to study the global non-linear dynamics.

Definition : An elementary catastrophe model* is a parametrised system of gradient-like differential equations, specified by four things :

(i) a parameter space C,

(ii) a state space X,

(iii) an energy function $H:C\times X \to \mathbb{R}$, and

(iv) a dynamic D on X, parametrised by C, that locally minimises H.

---

* In the language of [14] this is at structure level 2.

The function H determines the equilibrium manifold, $E \subset C \times X$, by the equation $\nabla_X H = 0$. The catastrophe map $\chi: E \to C$ is induced by projection. The bifurcation set is the image in C of the singularities of χ. If H is generic then E has the same dimension as C, and the only singularities of χ are elementary catastrophes, by the classification theorem [12,13].

We first construct the model for the 2-dimensional rolling problem only, where it is easy to understand and visualise, and then in subsequent sections extend it to 3-dimensions to include pitching, heaving and loading.

(i) Define the parameter space to be the plane C containing our 2-dimensional ship. The parameter $G \in C$ is the position of the centre of gravity of the ship (relative to the hull).

(ii) Define the configuration space to be the unit circle, S. The configuration of the ship is uniquely determined by the angle $\theta \in S$. Define the state space, $X = T^*S$, to be the cotangent bundle* of S. The state of the ship is given by $(\theta, \omega) \in T^*S$, where ω is the angular momentum. As before let

W = weight of ship

I = moment of inertia of ship and entrained water.

h = $h(G,\theta)$ = height of G above B_θ, at angle θ

= ZB_θ, in Figure 1(b)

Lemma 9.

The potential energy of the system is: $P = P(G,\theta) = Wh$.

The kinetic energy of the system is: $K = K(\omega) = \frac{\omega^2}{2I}$.

Proof.

Let h_1 = height of G above the water line,

h_2 = depth of B_θ below the water line.

---

* For a general treatment of Hamiltonians on cotangent bundles see [1].

Then taking the water line as zero potential,

Wh_1 = potential energy of the ship,

Wh_2 = potential energy of the displaced water.

Therefore P = total potential energy = $Wh_1 + Wh_2 = Wh$.

The angular momentum $\omega = I\dot{\theta}$, and therefore as required

$$K = \text{kinetic energy} = \frac{1}{2}I\dot{\theta}^2 = \frac{\omega^2}{2I} .$$

(iii) Define the energy function of the model to be the Hamiltonian $H: C \times T^*S \to \mathbb{R}$ given by

$$H = P + K = Wh + \frac{\omega^2}{2I}$$

We can now deduce the equilibrium surface and bifurcation set from H, as follows.

Lemma 10. $\dfrac{\partial h}{\partial \theta} = \ell$.

Proof. Let M_θ, ρ_θ be the centre and radius of curvature of $\mathcal{B}$ at B_θ. Let $\mu_\theta = GM_\theta$, $\alpha = G\hat{M}_\theta B_\theta$. Then

$$h(G,\theta) = \rho_\theta - \mu_\theta \cos\alpha$$

$$h(G,\theta+\varphi) = \rho_\theta - \mu_\theta \cos(\alpha+\varphi) + O(\varphi^2)$$

$$\frac{\partial h}{\partial \theta} = \left[\frac{\partial}{\partial \varphi} h(G,\theta+\varphi)\right]_{\varphi=0}$$

$$= \left[\mu_\theta \sin(\alpha+\varphi) + O(\varphi)\right]_{\varphi=0}$$

$$= \mu_\theta \sin\alpha = \ell .$$

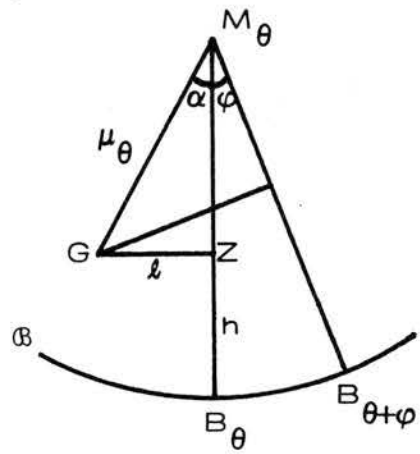

Figure 20.

The buoyancy locus $\mathcal{B}$ has coordinate θ, and is contained in the ambient space C. Therefore the normal bundle $N\mathcal{B}$ of $\mathcal{B}$ is defined by

$$N\mathcal{B} = \{N_\theta \times \theta\} \subset C \times S .$$

The geodesic spray is the natural map $N\mathcal{B} \to C$ of the normal bundle into the ambient space induced by projection $C \times S \to C$. The image of the singularities of the geodesic spray is the evolute of $\mathcal{B}$, which we have called the metacentric locus $\mathfrak{M}$.

Theorem 5. The equilibrium surface E is the normal bundle $N\mathcal{B}$ the buoyancy locus. The catastrophe map $\chi: E \to C$ is the geodesic spray. The bifurcation set is the metacentric locus, $\mathfrak{M}$.

Proof. E is given by $\nabla_X H = 0$, in other words by the equations

$$\frac{\partial H}{\partial \theta} = \frac{\partial H}{\partial \omega} = 0 \ .$$

Now $\frac{\partial H}{\partial \omega} = \frac{\omega}{I}$, and hence $\omega = 0$. Therefore $E \subset CxS \subset CxT^*S$, where S is identified with the zero-section of T^*S. Also $\frac{\partial H}{\partial \theta} = W\frac{\partial h}{\partial \theta} = W\ell$, by Lemma 10, and hence $\ell = 0$. Therefore $G \in N_\theta$, the normal to $\mathcal{B}$ at B_θ. Therefore

$$E = \{(G,\theta,0); G \in N_\theta\} = \{N_\theta x \theta\} = N\mathcal{B} \ .$$

The catastrophe map χ merely says "forget θ", mapping each normal to itself, and giving the geodesic spray. Hence the bifurcation set, which is defined to be the image of the singularities of χ, equals $\mathfrak{M}$. This completes the proof of Theorem 5. To complete the model there remains to define the dynamic.

Assuming G fixed, the Hamiltonian dynamic on T^*S is uniquely determined from H by the intrinsic symplectic structure of the cotangent bundle (Newton's law of motion is built-in [1]). Explicitly the dynamic is given by the Hamiltonian equations

$$\dot{\theta} = \frac{\partial H}{\partial \omega} = \frac{\omega}{I}$$
$$\dot{\omega} = -\frac{\partial H}{\partial \theta} = -W\frac{\partial H}{\partial \theta} = -W\ell \ .$$

Therefore

$$I\ddot{\theta} = \dot{\omega} = -W\ell \ .$$

which is the same as equation (1) in Section 2. The resulting Hamiltonian flow is the accurate global non-linear generalisation of the approximate local simple harmonic rolling solution (3). However as yet we have not included any friction, because the Hamiltonian flow is conservative, conserving the energy H.

(iv) Define the dynamic D of the catastrophe model to be the Hamiltonian dynamic with non-zero damping. There is no need to be

any more specific about the nature of the damping other than saying that energy is dissipated, because this ensures that H decreases along the orbits of D. Therefore H is a Lyapunov function for D. Therefore D locally minimises H, and depends upon the parameter G, as required. The model is complete.

11. GLOBAL DYNAMICS.

In order to understand the catastrophe dynamic D we fix G and draw the phase portrait of the resulting flow in Figure 21(c). The phase portrait is the family of orbits on T^*S. Since T^*S is a cylinder, we cut the cylinder along the generator $\theta = \pi = -\pi$, and lay it out flat, with the understanding that the two sides should be identified. In Figure 21 the dotted parts to the right of $\theta = \pi$ are merely the periodic repeats of the left hand sides of the portraits.

Before drawing the portrait of the damped flow, we first draw two portraits of the undamped Hamiltonian flow for two different positions of G in Figure 21(a) and (b). The latter is easier to understand because the Hamiltonian orbits are contained in the energy levels of H, which are themselves 1-dimensional since T^*S is 2-dimensional.

Figure 21(a) shows the Hamiltonian flow for G on the axis of symmetry below M, as in the case of the ship or the canoe in Figure 10. The 4 equilibria are given by $\omega = 0$ and

$\theta_2 = 0$, stable vertical

θ_1, θ_3, unstable capsizing angles (see Figure 12(b))

$\theta_4 = \pi$, stable turned turtle.

We are assuming that the ship does not sink if it capsizes, but is capable of floating upside down in stable equilibrium. The other three equilibria, $\theta_1, \theta_2, \theta_3$ correspond to the three points above G on the three sheets of E in Figure 11(b) for the canoe and

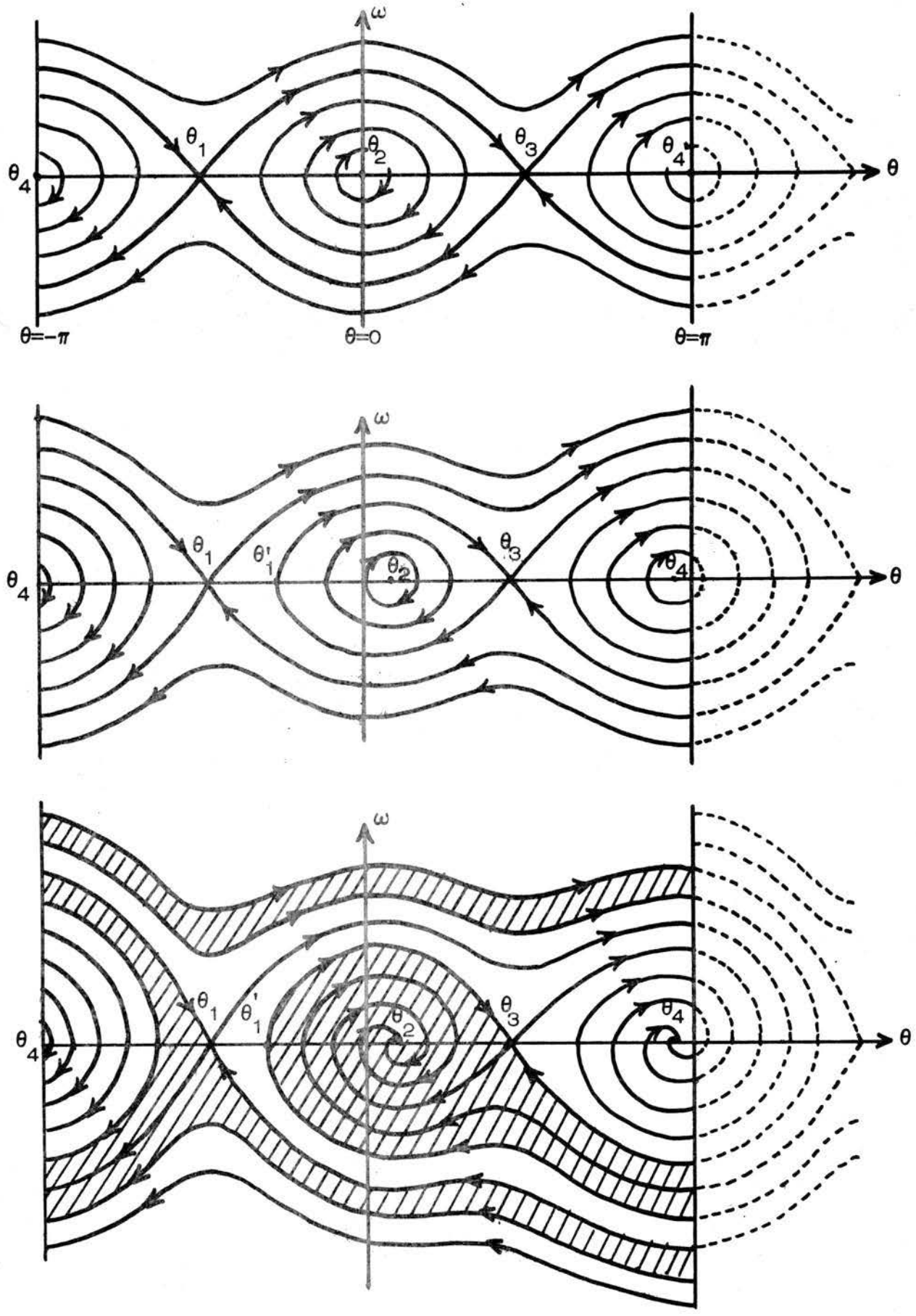

Figure 21. Phase portraits. *(a) Hamiltonian flow, G central.*
(b) Hamiltonian flow, G offset to right.
(c) Damped flow, G offset to right.

Figure 17(b) for the ship. The closed orbits round θ_2 represent rolling, as in the solution (3) of Section 2. The closed orbits round θ_4 represent rolling while turned turtle. The uppermost orbit going from left to right (which is closed since $\pi = -\pi$) represent the ship rolling over and over clockwise; the lowermost orbit represents the same but anticlockwise.

Figure 21(b) shows the Hamiltonian flow when G has been displaced slightly to the right. As a result, in stable equilibrium the ship will heel slightly to the right : $\theta_2 > 0$. Figures 11(b) and 17(b) show that the capsizing angles will also change slightly, θ_3 decreasing and $|\theta_1|$ increasing. Therefore it takes less energy to capsize to the right than to the left, because the θ_3-energy-level lies inside that of θ_1.

There is also a dynamic capsizing phenomenon, as follows. Let θ_1' be the intersection of the θ-axis with the θ_3-energy-level, such that $\theta_1 < \theta_1' < 0$. We call θ_1' the dynamic capsizing angle. If the ship is displaced to angle θ such that $\theta_1 < \theta < \theta_1'$, then it will not capsize to the left, but on the return roll to the right it will roll right over and then capsize, because the orbit will lie outside the θ_3-energy-level. Consequently, from the point of view of resonance, the dynamic capsizing angle is more dangerous than the static capsizing angle, because it is smaller

$$|\theta_1'| < \theta_3 < |\theta_1| .$$

On the other hand, if the ship rolls to the right almost as far as θ_3, then the recovery will take much longer, because, for small ε, the time to roll back from $\theta_3 - \varepsilon$ upright again will vary as $|\log \varepsilon|$, as can be seen by considering the linear approximation at θ_3. Therefore the ship will tend to hang perilously in the brink of capsizing for a long time, vulnerable to the chance wave or squall that might tilt her over the brink.

Figure 21(c) shows the damped flow for the same position of G. Since the dynamic is now dissipative the two stable equilibria

θ_2 and θ_4 are now attractors. If this figure was superimposed upon the figure above, all the damped orbits would cross the energy levels towards the attractors. The basin of attraction of the upright attractor θ_2 is shown shaded, and the complement is the basin of attraction of the turned turtle attractor θ_4. The capsizing angles are qualitatively unchanged since, being saddle-points of the Hamiltonian flow, they were already structurally stable. Similarly all the remarks about capsizing hold good.

Problem. What is the best way to introduce the effect of wind and wave into the model, so as to generalise the induced linear rolling of Section 4 to the non-linear situation? The effect of periodic waves can be simulated by introducing a new cyclic parameter that translates the phase-portrait to and fro parallel to the θ-axis, corresponding to adding a forcing term representing the varying water surface, as in Figure 5 and equation (9). The induced roll is then an attracting closed orbit lying over the parameter-cycle. Perhaps the effect of the wind could be similarly modelled by translating the phase-portrait parallel to the ω-axis, to simulate the impulse transmitted by the wind into angular momentum.

12. MODEL INCLUDING PITCHING.

We first enlarge the model to 3-dimensions to incorporate pitching as well as rolling, as follows.

(i) The parameter space for G is now 3-dimentional, $C = \mathbb{R}^3$.

(ii) The configuration space is now the unit sphere, $S = S^2$. The configuration of the ship is uniquely determined by the spherical coordinate $\theta \in S$. The state space is the cotangent bundle, $X = T^*S$, which is now a non-trivial 4-dimensional bundle. The state is given by $(\theta,\omega) \in T^*S$, where $\omega \in T^*_\theta S$ now represents the horizontal component of angular momentum at θ (the vertical yawing

component of angular momentum is automatically excluded - see Lemma 12 below).

(iii) The energy is the Hamiltonian $H = P+K$, where the potential energy $P = Wh$, exactly as before. Meanwhile the kinetic energy $K = K_\theta(\omega)$ is the usual quadratic form on $T^*_\theta S$, defined as follows. If $(\omega_1,\omega_2,\omega_3)$ are coordinates of ω relative to the principal axes of inertia of the ship (which are tilted by θ), and (I_1,I_2,I_3) are the corresponding moments of inertia, then

$$K_\theta(\omega) = \Sigma\, \omega_i^2/2I_i \ .$$

(iv) As before, the dynamic is the damped Hamiltonian dynamic, and this completes the 3-dimension model.

Theorem 6. Theorem 5 holds for the 3-dimensional model.

Proof. E is defined by $\nabla_\theta H = \nabla_\omega H = 0$. Since the kinetic energy $K_\theta(\omega)$ is positive definite in ω, $\nabla_\omega H = \nabla_\omega K = 0$ implies $\omega = 0$. Therefore $E \subset C\times S$ as before.

Let Figure 20 represent the vertical plane through G and B_θ. Although θ is now a spherical coordinate, we can still define the angle α, and give meaning to $\theta+\varphi$, where φ is an angle. As in the proof of Lemma 10,

$$\left[\frac{\partial}{\partial\varphi}h(G,\theta+\varphi)\right]_{\varphi=0} = \ell \ .$$

$$\nabla_\theta H = 0 \Longrightarrow \nabla_\theta h = 0$$
$$\Longrightarrow \text{left-hand side vanishes}$$
$$\Longrightarrow \ell = 0$$
$$\Longrightarrow G \in N_\theta$$
$$\Longrightarrow E = N\mathfrak{B}, \text{ as required.}$$

The rest of the Theorem follows naturally, as before.

The geometry of the 3-dimensional model is more complicated, for this time E is a 3-manifold folded over $\mathfrak{M}$, and $\mathfrak{M}$ is a surface with cusped edges and singular points. In particular, as the ship pitches, the rolling metacentre M traces out a curve on $\mathfrak{M}$, which

we call the pitching curve, $\mathfrak{P}$, and which, due to the bilateral symmetry of the ship, is a cusped edge of $\mathfrak{M}$ containing various singular points. In an ellipsoidal ship $\mathfrak{B}$ is a similar ellipsoid, and $\mathfrak{P}$ is an ellipse containing 4 hyperbolic umbilics, and these are the only singular points of $\mathfrak{M}$ (see [5]). For any floating shape, $\mathfrak{M}$ always has at least 4 hyperbolic umbilics, because, by counting indices, the number of hyperbolic umbilics minus the number of elliptic umbilics is twice the Euler characteristic of $\mathfrak{B}$, which is 2.

In a wall-sided ship there are 4 other singular points on $\mathfrak{P}$, namely 4 unbiased-butterflies, where the butterfly sections (shown in Figures 16 and 17) bifurcate back into single cusps fore and aft. These butterfly points explain why large pitching enhances the danger of capsizing, because if the pitching angle passes beyond them then the rolling-capsizing-angle decreases. In other words pitching has the same qualitative effect as isotoping a ship-shaped section into a canoe-shaped section (see the Problem after Theorem 3 Remark 3), and the resulting decrease in capsizing angle can be seen by comparing Figures 12(b) and 17(a). Moreover large pitching can occur at the same time as resonant rolling, if the ship is less than half the wave-length and steers a sensitive course (see Section 5 and Figure 7). Therefore the geometry of the butterfly may be relevant to the study of capsizing of small vessels in heavy seas. Of the 13 merchant ships that were known to have capsized and sunk during 1975, 11 were small cargo or fishing vessels of 350 tons or less [10]. In Section 14 below we discuss the effect on the capsizing angles of heaving, or having the crest of a wave amidships.

13. MODEL INCLUDING HEAVING.

Next we enlarge the model to incorporate heaving. The enlarged model automatically contains all the coupling between the three modes of oscillation, rolling, pitching and heaving.

(i) As before, the parameter space is $C = \mathbb{R}^3$.

(ii) The configuration of the ship is given by $(\theta,q) \in S\times\mathbb{R}$ where θ is the spherical coordinate, and q the vertical coordinate of heaving. Let $B_{\theta,q}$ denote the resulting centre of buoyancy. The state is given by

$$(\theta,q,\omega,p) \in T^*(S\times\mathbb{R}),$$

where p denotes the vertical linear momentum and ω is as before.

(iii) The potential energy is given by

$$P = p(G,\theta,q) = Wh_1 + Vh_2,$$

where h_1 = height of G above water line
h_2 = depth of $B_{\theta,q}$ below water line
V = weight of water displaced
} all functions of θ,q.

The kinetic energy is given by

$$K = K_\theta(\omega) + K(p) = \Sigma\, \omega_i^2/2I_i + gp^2/2W \quad .$$

As before the energy

$$H : C\times T^*(S\times\mathbb{R}) \longrightarrow \mathbb{R}$$

is the Hamiltonian, $H = P+K$, and the dynamic is the damped Hamiltonian dynamic. We define the buoyancy locus to be the same as before, consisting only of those centres of buoyancy for which there is no heaving,

$$B = \{B_\theta\} = \{B_{\theta,q};\ q=0\} \ .$$

Theorem 7. Theorem 5 holds.

Proof. E is given by $\nabla_\theta H = \nabla_\omega H = \frac{\partial H}{\partial q} = \frac{\partial H}{\partial p} = 0$. Now $\frac{\partial H}{\partial p} = \frac{gp}{W}$, and so $p = 0$. We shall show $\frac{\partial H}{\partial q} = 0$ implies $q = 0$. Hence the problem reduces to the previous case, $E \subset C\times S$, and the result follows from Theorem 6. Let

$k_i = h_i(\theta,0)$
$U = W - V$.
u = height of centre of emerged slice above water line.

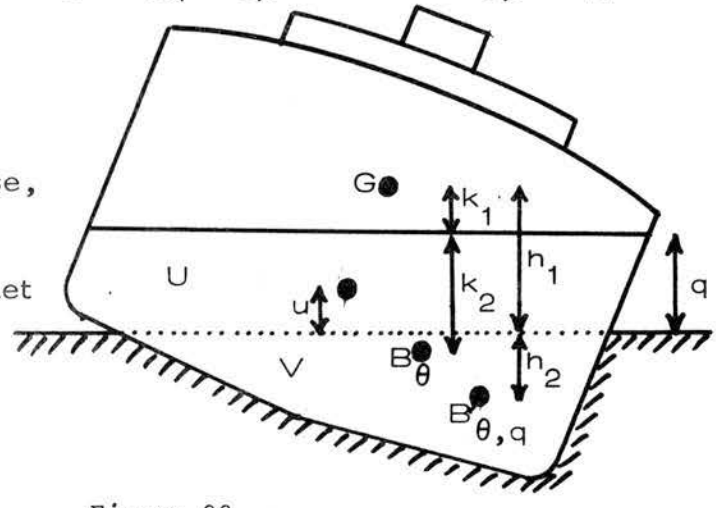

Figure 22.
Heaving, while rolling and pitching.

Then $h_1 = k_1 + q$.

By taking moments of the displaced water about the water-line,

$$W(k_2-q) = Vh_2 - Uu \ .$$

Therefore

$$P = Wh_1 + Vh_2 = W(k_1+q) + W(k_2-q) + Uu$$
$$= W(k_1+k_2) + Uu \ .$$

Therefore

$$\frac{\partial H}{\partial q} = \frac{\partial P}{\partial q} = \frac{\partial U}{\partial q}u + U\frac{\partial u}{\partial q} \text{ , since } k_1 + k_2 \text{ independent of } q.$$

From Figure 22,

$$U,u \gtrless 0 \text{ as } q \gtrless 0, \text{ and } \frac{\partial U}{\partial q} \geq 0, \ \frac{\partial u}{\partial q} > 0.$$

Therefore

$$\frac{\partial H}{\partial q} \gtrless 0 \text{ as } q \gtrless 0.$$

Therefore

$$\frac{\partial H}{\partial q} = 0 \text{ implies } q = 0, \text{ as required.}$$

Lemma 11. For small heaving while upright the Hamiltonian dynamic reduces to the linear theory.

Proof. In the case of a wall-sided ship of draught D we have approximately

$$U = \frac{Wq}{D} \ , \ u = \frac{q}{2} \ , \text{ and therefore } Uu = \frac{Wq^2}{2D} \ .$$

The Hamiltonian equations give

$$\dot{q} = \frac{\partial H}{\partial p} = \frac{gp}{W} \ , \ \dot{p} = -\frac{\partial H}{\partial q} = -\frac{\partial}{\partial q}(Uu) = \frac{Wq}{D}$$

Therefore $\ddot{q} = \frac{g}{D}q$, as in equation (17) of Section 6.

14. MODEL INCLUDING LOADING.

Finally we enlarge the model to incorporate loading by allowing the weight of the ship to act as another parameter. At the same time we place the treatment in a more elegant group-theoretical setting.

(i) The parameter is (W,G), where W is the weight and G the centre of gravity. The condition for the ship to float is $W \in \overline{W}$, where $\overline{W}$ denotes the open internal $0 < W < \mathcal{W}$, and $\mathcal{W}$ is the weight that would just sink it. Therefore the parameter space is 4-dimensional, $C = \overline{W} \times \mathbb{R}^3$.

(ii) Let $\mathcal{G}$ be the 6-dimensional group of Euclidean motions in $\mathbb{R}^3$. Choose an arbitrary reference position of the ship, and let $\mathcal{G}$ act on this reference position by right action. The potential energy of the water displaced is determined by $g \in \mathcal{G}$, and the potential energy of the ship determined by g and the parameter (W,G), as in the last section. The kinetic energy is the classical positive definite quadratic on $T^*\mathcal{G}$ for a rigid body. The sum gives the Hamiltonian

$$H : C \times T^*\mathcal{G} \longrightarrow \mathbb{R}.$$

Remark 1. The kinetic energy depends not only upon the weight but also upon the inertia tensor I of the ship. Therefore both H and the dynamic depend on I, which we could take as another 6-dimensional parameter. However in equilibrium the kinetic energy vanishes, and so I does not affect the equilibrium manifold. Therefore to identify the latter it is not necessary to specify I, which can be arbitrary.

Remark 2. The above H is no good for a catastrophe potential because it is not generic, and would give a 7-dimensional equilibrium manifold, which is 3 dimensions too big. We therefore need to factor out by the symmetries of H, as follows. $\mathcal{G}$ acts on the left of $T^*\mathcal{G}$ by :

$$h(g,t) = (hg,(T^*_g h)^{-1} t), \quad h \in \mathcal{G},\ g \in \mathcal{G},\ t \in T^*_g\mathcal{G} ,$$

and hence on the right of H by :

$$(Hh)(c,g,t) = (c,h(g,t)) .$$

Define the symmetry group

$$\mathrm{Sym}(H) = \{h \in \mathcal{G};\ Hh = H\} .$$

Let $\mathfrak{H}$ be the 3-dimensional subgroup of $\mathfrak{G}$ preserving the horizontal (consisting of horizontal translations and rotations about vertical axes).

Lemma 12. Sym (H) = $\mathfrak{H}$.

Proof. The action of $\mathfrak{G}$ does not affect kinetic energy, and so we are only concerned with potential energy. $\mathfrak{H}$ does not alter potential energy and so $\mathfrak{H} \subset$ Sym(H). Conversely Sym(H) $\subset \mathfrak{H}$, because $\mathfrak{G}/\mathfrak{H}$ is spanned by the 1-parameter subgroups of rolling, pitching and heaving, which do alter H by the proof of Theorems 6 and 7.

We can now construct the model. Define the state space to be $(T^*\mathfrak{G})/\mathfrak{H}$, which is a 6-vector bundle over the 3-manifold $\mathfrak{G}/\mathfrak{H}$. In other words the state of the ship is determined by its 6 coordinates of momentum and its 3 coordinates of roll, pitch and heave (while its other 3 coordinates of latitude, longitude and course are automatically ignored). Define the potential to be the induced Hamiltonian

$$H : C \times (T^*\mathfrak{G})/\mathfrak{H} \longrightarrow \mathbb{R} .$$

Define the dynamic to be the damped Hamiltonian dynamic. This completes the model, and we now proceed to identify the equilibrium manifold E.

As before let S denote the unit sphere. Let

$$\theta : \mathfrak{G}/\mathfrak{H} \longrightarrow S$$

denote the projection given by defining $\theta(\mathfrak{H}g)$ to be the direction of the image of the vertical under g. (This is well-defined since $\mathfrak{H}$ preserves the horizontal, and hence also the vertical).

Each $W \in \overline{W}$ determines a buoyancy locus $\mathfrak{B}^W \subset \mathbb{R}^3$. As W varies from 0 to W, $\{\mathfrak{B}^W\}$ is a decreasing nested family of convex closed surfaces filling the convex hull of the ship's hull, running from the boundary B^0 to the single point $\mathfrak{B}^W$ at the submerged centre of buoyancy.

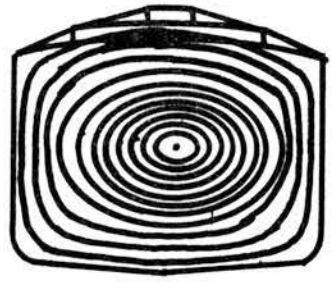

Figure 23. Buoyancy loci $\{\mathfrak{B}^W\}$.

For each W, $\mathfrak{B}^W$ has evolute $\mathfrak{M}^W$, normal bundle $N\mathfrak{B}^W$, and geodesic spray

$$N\mathfrak{B}^W = \{N_\theta^W \times \theta\} \xrightarrow{\subset} \mathbb{R}^3 \times S \xrightarrow{\text{proj}} \mathbb{R}^3 .$$

Define the complete buoyancy locus to be the 3-manifold

$$\mathfrak{B} = \{W \times \mathfrak{B}^W\} \subset \overline{W} \times \mathbb{R}^3 = C ,$$

with complete metacentric locus,

$$\mathfrak{M} = \{W \times \mathfrak{M}^W\} \subset C$$

and complete normal bundle and geodesic spray

$$N\mathfrak{B} = \{W \times N\mathfrak{B}^W\} \xrightarrow{\subset} C \times S \xrightarrow{\text{proj}} C .$$

Theorem 8. θ induces a diffeomorphism from the equilibrium manifold E onto the complete normal bundle $N\mathfrak{B}$ such that the diagram is commutative.

$$\begin{array}{ccc} E & \xrightarrow{\cong} & N\mathfrak{B} \\ \downarrow \subset & & \downarrow \subset \\ C \times \mathfrak{G}/\mathfrak{H} & \xrightarrow{1\times\theta} & C \times S \end{array}$$

Therefore the catastrophe map $\chi: E \to C$ is equivalent to the geodesic spray $N\mathfrak{B} \to C$, and the bifurcation set is the complete metacentric locus $\mathfrak{M}$.

Proof. Since kinetic energy is positive definite, equilibria lie in the zero section $\mathfrak{G}/\mathfrak{H}$ of the state space $(T^*\mathfrak{G})/\mathfrak{H}$. Fix W, and let E^W denote the corresponding section of the equilibrium manifold. Let φ^W denote the diffeomorphism

$$\varphi^W : \mathbb{R}^3 \times \mathfrak{G}/\mathfrak{H} \longrightarrow \mathbb{R}^3 \times S \times \mathbb{R}$$

$$(G, \mathfrak{H}g) \longmapsto (G, \theta, q) ,$$

where $\theta = \theta(\mathfrak{H}g)$ and q is the height of Gg above the level that G would be at angle θ, were a weight W of water displaced. (This is well defined since $\mathfrak{H}$ preserves that level). Then $\varphi^W E^W = N\mathfrak{B}^W \times 0$ by Theorem 6. Therefore there are diffeomorphisms :

$$\begin{array}{ccccc} E^W & \xrightarrow{\cong} & N\mathfrak{B}^W \times 0 & \xrightarrow{\cong} & N\mathfrak{B}^W \\ \downarrow \subset & & \downarrow \subset & & \downarrow \subset \\ \mathbb{R}^3 \times \mathfrak{G}/\mathfrak{H} & \xrightarrow[\cong]{\varphi^W} & \mathbb{R}^3 \times S \times \mathbb{R} & \xrightarrow{\text{project}} & \mathbb{R}^3 \times S \end{array}$$

Premultiplying by W, and taking the union for all $W \in \overline{W}$, give the result. Projecting onto C yields the required equivalence.

$$\begin{array}{ccc} E & \xrightarrow{\cong} & N\mathfrak{B} \\ \chi \downarrow & & \downarrow \text{geodesic spray} \\ C & \xrightarrow{1} & C \end{array}$$

Both sides have the same image of singularities, and hence the bifurcation set is $\mathfrak{M}$. This completes the proof of Theorem 8.

Theorem 9. The metacentric loci $\mathfrak{M}^W$ and $\mathfrak{M}^{\mathcal{W}-W}$ are similar. $\mathfrak{M}^W$ is obtained by reflecting $\mathfrak{M}^{\mathcal{W}-W}$ in the submerged buoyancy centre $\mathfrak{B}^{\mathcal{W}}$ and scaling by $\frac{\mathcal{W}-W}{W}$.

Proof. Let V_θ^W denote the volume displaced by weight W at angle θ. Then the volume of the ship can be written as a disjoint union

$$V^{\mathcal{W}} = V_\theta^W \cup V_{T\theta}^{\mathcal{W}-W}$$

where T is the antipodal map of S. Therefore the buoyancy centre B_θ^W is obtained by reflecting $B_{T\theta}^{\mathcal{W}-W}$ in $B^{\mathcal{W}}$ and scaling by $\frac{\mathcal{W}-W}{W}$. Therefore this similarity maps B^W to $B^{\mathcal{W}-W}$, and hence $\mathfrak{M}^W$ to $\mathfrak{M}^{\mathcal{W}-W}$.

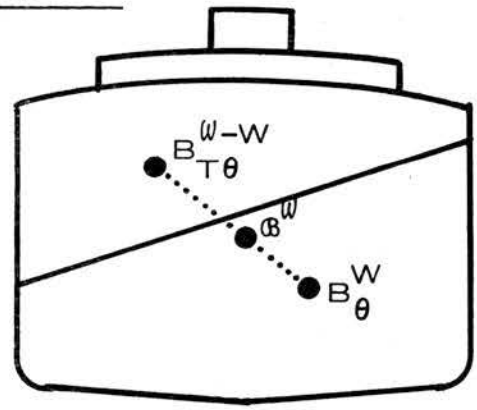

Figure 24.

Corollary 1. $\mathfrak{M}^{\mathcal{W}/2}$ is symmetrical about $\mathfrak{B}^{\mathcal{W}}$.

Corollary 2. $\mathfrak{M}^{3\mathcal{W}/4}$ is one third the size of $\mathfrak{M}^{\mathcal{W}/4}$.

The Corollaries are illustrated in Figure 25 for a typical 2-dimensional section of a ship having beam:draught ratio = 3 when $W = \mathcal{W}/2$. The position of G is fixed, and the properties are the same as those of the liner in Section 2. The metacentric locus in Figure 25(b) has 8 cusps, and when the weight increases or decreases 4 swallowtails appear creating 8 more cusps, 16 in all.

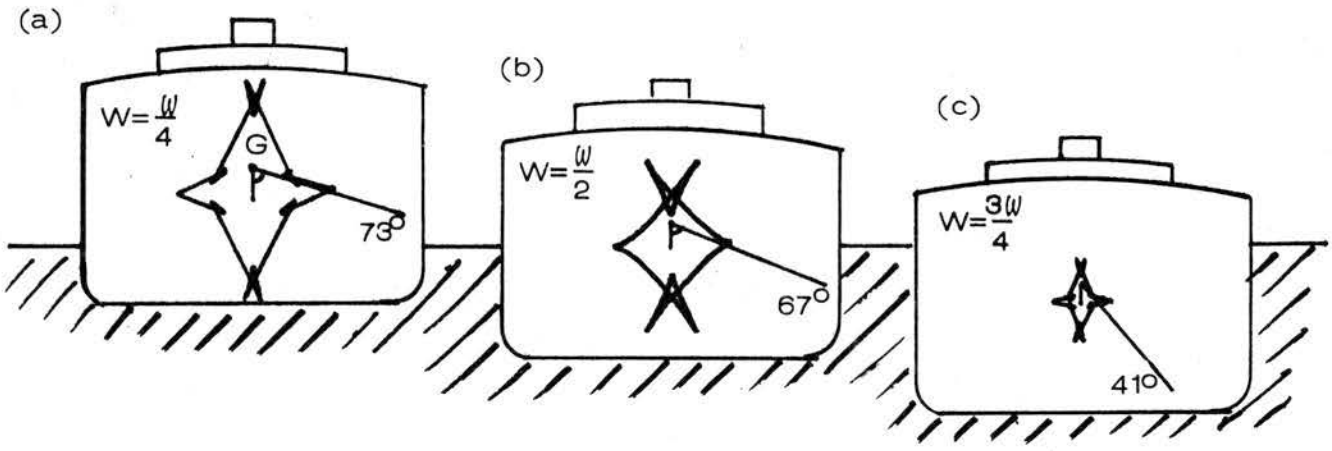

Figure 25. Decrease in size of $\mathfrak{M}^W$, and capsizing angle, with weight.

As the weight increases the ship becomes more susceptible to capsizing, not only because the bifurcation set shrinks closer to G, but also because the capsizing angle drops dramatically. The latter is caused by the appearance of the swallowtails. Figure 26 shows graphs of metacentric height and capsizing angle as functions of W, assuming G fixed. The dynamic capsizing angle can drop even further if there is a shift of cargo (see Figure 21).

This geometry is also relevant to the capsizing of small ships in following seas (small means the ship length is less than the wave-length), for when the crest of the wave is amidships, the buoyancy amidships carries more of the weight.

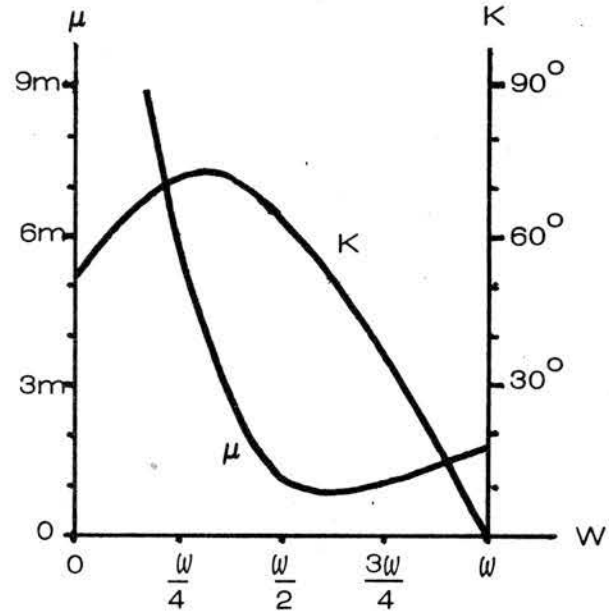

Figure 26. Metacentric height μ and capsizing angle K as functions of weight W.

Therefore although the ship may be designed as in Figure 25(b), she may unwittingly find herself riding on the crest of a wave as in Figure 25(c). The usual approach of linear theory is to emphasise the loss of stability due to the loss of metacentric height [9], but Figure 26 suggests that the non-linear drop in capsizing angle may in fact be more dangerous. A similar phenomenon may occur in a head sea, if the high frequency of encountered waves happens to resonate with heaving.

We conclude by considering the loading of cargo onto the ship. As W increases G may move, and so the parameter (W,G) follows a path p in the parameter space C. If p crosses $\mathfrak{M}$ the ship may heel, or right itself, or capsize. To illustrate this consider two such loading paths shown in Figure 27. The weight of the ship is $\mathcal{W}/6$ when empty and $5\mathcal{W}/6$ when full. During path p_1 the cargo is stowed so as to keep G fixed at the centre $\mathcal{B}^{\mathcal{W}}$ of the ship, whereas during p_2 the cargo is loaded from the bottom upwards, as in a tanker. Meanwhile the dotted line shows how the height of the metacentre M^W depends upon W. The latter is drawn for a narrow ship, (with beam:draught ratio = 2 when $W = \mathcal{W}/2$.) because the narrowness lowers the path of M^W so as to cut p_1. Therefore p_1 suffers the two catastrophes of heeling and righting, whereas p_2 suffers none because it skirts below the dotted line.

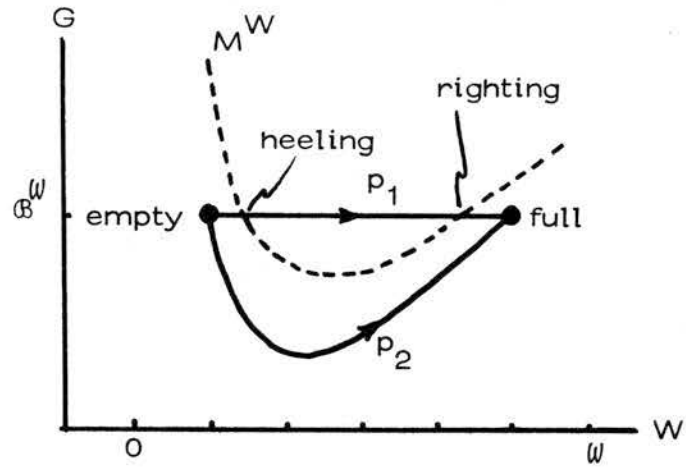

Figure 27. Two loading paths.

The corresponding behaviour of the ship is illustrated in Figure 28. In each case the metacentric locus $\mathfrak{M}^W$ is sketched,

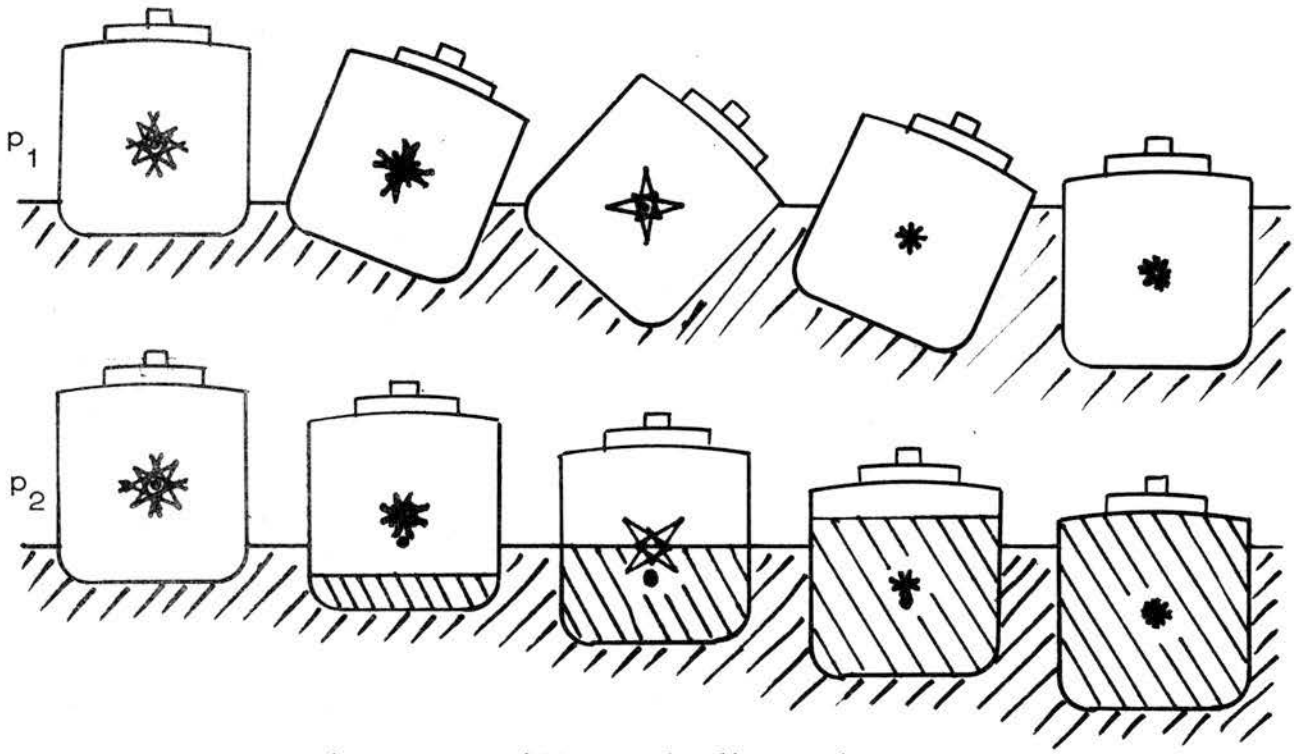

Figure 28. Different loading paths.

and G is indicated by a blob. Certain heavy narrow old cargo boats have a loading path like p_2, but the heaviness of the empty boat displaces the empty position in Figure 27 to the right across the dotted line; therefore such a boat heels with negative metacentric height when empty, and then suddenly rights itself during loading. If there is not enough cargo then the boat must take on ballast before sailing.

15. CONCLUSION

Could this geometrical approach to be **of any practical use**? It is difficult to say at this stage, but we tentatively suggest two areas for further exploration. Firstly the singularities involved are stable and qualitatively simple phenomena, sitting halfway between the geometric complexity of the shape of the ship and the dynamic

complexity of its behaviour in the seaway. If details of a number of individual ships were analysed in the light of these singularities, it might give some further insight into how design can influence performance, and eventually might even suggest more sophisticated stability criteria.

Secondly there is at present a lack in the theory of non-linear coupling. Consequently there is a lack of mathematical language in which to express and communicate the intuition, which experienced pilots possess, of how to handle a ship in heavy weather. It is not enough to say that capsizing is probably due to that one-in-a-million freak wave, because capsizings do occur more frequently than we would wish [10], and it might be that the intuitive knowledge of one experienced pilot could have saved another. A case in point is Lindemann's discovery of how to get out of a flat spin in an aircraft, by pushing the stick fully forward and kicking hard on the opposite rudder. What was at one time a situation dreaded by all fliers, is now a routine recovery procedure taught to all beginners. Analogously in ship stability, the qualitative simplicity of the singularities that we have been discussing might eventually lead to a better understanding of the routine procedures for handling that freak wave.

REFERENCES.

1. R. Abraham & J.E. Marsden, Foundations of mechanics, Benjamin, New York, 1967.

2. K.C. Barnaby, Basic naval architecture, Hutchinson, London, 1963.

3. S.N. Blagoveshchensky, Theory of ship motions (English trans.), Dover, New York, 1962.

4. P. Bouguer, Traite du Navire, de sa construction et de ses mouvements, Paris, 1746.

5. A. Cayley, On the centro-surface of an ellipsoid, Trans. Camb. Phil. Soc. 12 (1873) 319-365.

6. G. Durrell, My family and other animals, Penguin, England, 1956.

7. L. Euler, Scientia Navalis, St. Petersburg, 1749.

8. P.J. Holmes & D.A. Rand, The bifurcations of Duffing's equation : and application of catastrophe theory, J. Sound & Vib, 44 (1976) 237-253.

9. C. Kuo, International Conference on Stability of Ships and Ocean vehicles, University of Strathclyde, Glasgow 1975.

10. Lloyd's Register of Shipping, Casualty Return, Lloyd's, London 1975.

11. A.M. Robb, Theory of Naval Architecture, Griffin, London, 1952.

12. R. Thom, Structural stability and morphogenesis, (trans : D D.H. Fowler), Benjamin, New York, 1975, (French edition 1972)

13. D.J.A. Trotman & E.C. Zeeman, The classification of elementary catastrophes of codimension ≤ 5, Structural stability, the Theory of catastrophes, and Applications in the Sciences, Springer Lecture Notes in Math. 525 (1976) 263-327.

14. E.C. Zeeman, Levels of structure in catastrophe theory, Proc. Int. Cong. Math. Vancouver (1974) 2, 533-546.

15. E.C. Zeeman, Duffing's equation in brain modelling, Bull. Inst. Math. & Appl., 12 (1976), 207-214.